13

Challenges and Solutions in Received Signal Strength-Based Seamless Positioning

Pedro Figueiredo e Silva, Philipp Richter, Jukka Talvitie, Elina Laitinen, Elena Simona Lohan

LABORATORY OF ELECTRONICS AND COMMUNICATIONS ENGINEERING, TAMPERE UNIVERSITY OF TECHNOLOGY, TAMPERE, FINLAND

1 Introduction and Definitions

According to Webster dictionary, seamless means "having no awkward transitions, interruptions, or indications of disparity" and it is often used synonymously with "smooth" and "continuous." One of the first papers to discuss in detail which are some possible mechanisms to attain a seamless positioning on mobile devices has been published in Sun et al. (2005). The authors in Sun et al. (2005) identified five main directions of research to help in creating seamless positioning platforms, namely: (i) data fusion approaches, (ii) single-step localization solutions, which nowadays can be translated into Simultaneous Localization and Mapping (SLAM) solutions (Taylor et al., 2011), (iii) use of smart antennas and Angle of Arrival (AOA) techniques, (iv) designing the network topologies with positioning in mind (unlike the classical approach where the network topology is designed fully according to communication targets), and (v) interoperability at positioning level, such as systems (cellular, WLAN, etc.) designed to include interoperable positioning features that can be then smoothly and easily accessed and combined.

Seamless positioning targets often go hand in hand with the targets of low-power consumption at the mobile side and the need of low-cost solutions at the network side. Interoperability of different positioning systems is also an important design criterion. Low-cost, low-power, and interoperable solutions can be usually achieved when there is no need of additional infrastructure or hardware updates and the localization is done based on available signals and infrastructures. This is why, the Received Signal Strength (RSS) solutions are one of the gaining techniques in the realm of low-cost, low-power, seamless, and interoperable positioning, and they form the core of this chapter.

Geographical and Fingerprinting Data for Positioning and Navigation Systems. https://doi.org/10.1016/B978-0-12-813189-3.00013-7

The RSS-based approaches can be basically used with any radio frequency (RF) communication systems whose standard supports RSS measurements or reporting. For example, cellular, WLAN, Bluetooth Low Energy (BLE), Radio Frequency Identification (RFID) are all systems which currently support RSS measurements or enable some form of RSS indication, and thus can be used for RSS-based positioning. The RSS-based positioning typically relies on fingerprinting techniques, involving two stages:

1. A training stage, where data about the environment, such as RSS measurements, are collected with different labels or position tags and stored into a training database available at the Location Service Provider (LSP) side, and
2. An estimation stage, where the mobile gets access to the full or partial information stored into the training database by the LSP and computes its position by matching the real-time RSS measurements with the measurements stored in the training database. This matching (or fingerprinting) process outputs a location label or a position, according to what was initially stored in the database.

One-stage approaches are also possible with RSS-based positioning, but they are much less accurate than the two-stage fingerprinting approaches. In the one-stage approaches, the receiver has to assume that a certain statistical path-loss model is valid in the location area. With an underlying path-loss model, and assuming that the transmitter location is known, an user receiving RSS measurements from three or more transmitters (or Access Nodes) in range can compute its most likely position.

The different types of RSS-based positioning via fingerprinting are described in Section 2.

2 Overview of Fingerprinting Methods

Following the discussion in the previous section, we can classify the RSS-based fingerprinting methods as shown in Fig. 1. The two-stage approaches are described in more detail in what follows. The path-loss (PL) probabilistic techniques can be used in both two-stage and one-stage approaches. The SLAM techniques are not covered in this chapter. For good surveys of SLAM techniques, the readers are referred to Agarwal et al. (2014) and Cadena et al. (2016).

2.1 Methods With Full Training Databases

The classical fingerprinting with a full training database refers to the two-stage approach where RSS measurements are first collected at different locations in a building and stored into a training database under the following quadruplet per access point $(P_{a,i}, x_i, y_i, z_i)$, where $P_{a,i}$ is the RSS value measured from the ath Access Point (AP) in the ith location in the building, and x_i, y_i, z_i are the 3D coordinates at the ith location. If an access point is not heard at a certain location, its RSS is set according to a convention. For example, in a Matlab-based analysis, we can use the convention that $P_{a,i} =$ NaN (Not A Number) if the

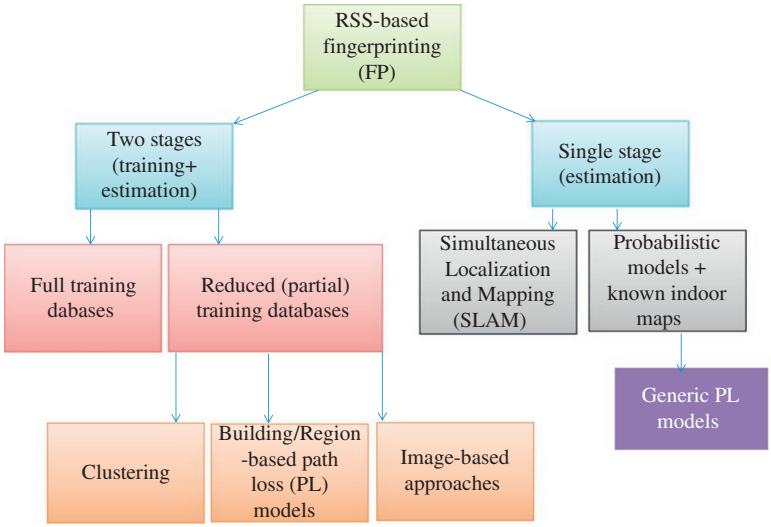

FIG. 1 Classification of fingerprinting approaches.

ath access point is not heard in that particular point. Alternatively, one can set the missing $P_{a,i}$ values to something very small, such as -200 dB, or simply ignore it.

Let us denote by N_{AP} the number of AP in the building and by N_m the number of measurement points or locations. In the estimation phase, the mobile measures the RSS $O_a, a = 1, \ldots, N_{AP}$ from the hearable access points in its range and compares the observed O_a RSS values with the $P_{a,i}$ values stored in the fingerprint database. We use the convention that $O_a = \text{NaN}$ if the ath access point is not heard by the mobile. The comparisons are done in terms of some metrics M_i, shown for example, in Table 1 and computed in each of the N_m measured locations. In Table 1, $\mathbf{O} = [O_1, O_2, \ldots, O_{N_{AP}}]^T$, $\mathbf{P}_i = [P_{1,i}, P_{2,i}, \ldots, P_{N_{AP},i}]^T$, and $S = \text{diag}(\sigma_1^2, \sigma_2^2, \ldots, \sigma_{N_{AP}}^2)$, where σ_a^2 is the noise variance per measured RSS in the ath AP. In each row of Table 1, only the commonly heard AP between the training database and the mobile's measurement are considered, according to the mentioned conventions. The choice of how to encode that information depends on these metrics, because they process that information differently (Torres-Sospedra et al., 2015) and not all combinations are feasible.

2.2 Methods With Reduced Training Databases

In order to store a lower number of parameters in the training database instead of all measured RSS values from all heard AP, several methods are available, such as clustering or classification (Cramariuc et al., 2016; Abdou et al., 2016), statistical path-loss modeling, compression or image-based (Talvitie et al., 2016), compressed sensing (Feng et al., 2012), feature extraction (Lin and Chen, 2016), principal component analysis (Mo et al., 2015),

Table 1 Examples of RSS Distance Metrics Used in Fingerprinting

Method	Metric M_i	Comparison Criterion
Euclidean	$M_i = \left(\sum_{a=1}^{N_{AP}} \|\|O_a - P_{a,i}\|\|^2 \right)^{1/2}$	$\min_i(M_i)$
Square of Euclidean (Spearman distance)	$M_i = \sum_{a=1}^{N_{AP}} \|\|O_a - P_{a,i}\|\|^2$	$\min_i(M_i)$
Manhattan distance	$M_i = \sum_{a=1}^{N_{AP}} \|\|O_a - P_{a,i}\|\|$	$\min_i(M_i)$
Mahalanobis distance	$M_i = \sqrt{(\mathbf{O} - \mathbf{P}_i)^T S^{-1} (\mathbf{O} - \mathbf{P}_i)}$	$\min_i(M_i)$
Logarithmic Gaussian likelihood	$M_i = \sum_{a=1}^{N_{AP}} \log \left(\frac{1}{\sqrt{2\pi\sigma_a^2}} e^{\left(-\frac{(O_a - P_{a,i})^2}{2\sigma_a^2} \right)} \right)$	$\max_i(M_i)$

etc. The main approaches to reduce a training database are explained in the following subsections.

2.2.1 Clustering Methods

Fig. 2 shows a classification of clustering approaches which can be used to decrease the size of the training database. Basically, the clustering or database reduction can be done either in coordinates domain (2D or 3D modeling), or in RSS or AP domain, but combined or hierarchical methods are also possible, for example, those based on Support Vector Machines (SVM) as reported in Khullar and Dong (2017). For example, the 3D coordinates clustering was compared with RSS clustering in Cramariuc et al. (2016) and it has been shown that the 3D coordinate clustering gives typically better positioning accuracy than the RSS clustering, at the expense of a higher computational complexity. Affinity propagation clustering combined with SVM has been studied, for example, in Abdou et al. (2016) for the purpose of keeping only the relevant AP in the location estimation and to achieve a low complexity algorithm implementation. This problem is also related with the AP reduction problem, addressed in Section 3.2.2.

2.2.2 Path-Loss Approaches

The path-loss (PL) approaches are another set of methods which can be used to reduce the size of the training databases. They rely on the assumption that each AP in a network obeys a certain, intrinsic path-loss propagation model, characterized by a set of few parameters, which can be modeled statistically. The most encountered PL model is the one-slope PL model, where the measured RSS in dB scale $P_{a,i}$ is given by:

$$P_{a,i} = P_{T_a} - 10 n_a \log(d_{a,i}) + \eta_{a,i},$$

where P_{T_a} is an "apparent" transmit power (in dB) of the ath AP in the network (typically measured at 1 m away from the AP), n_a is a path-loss (constant) coefficient characterizing

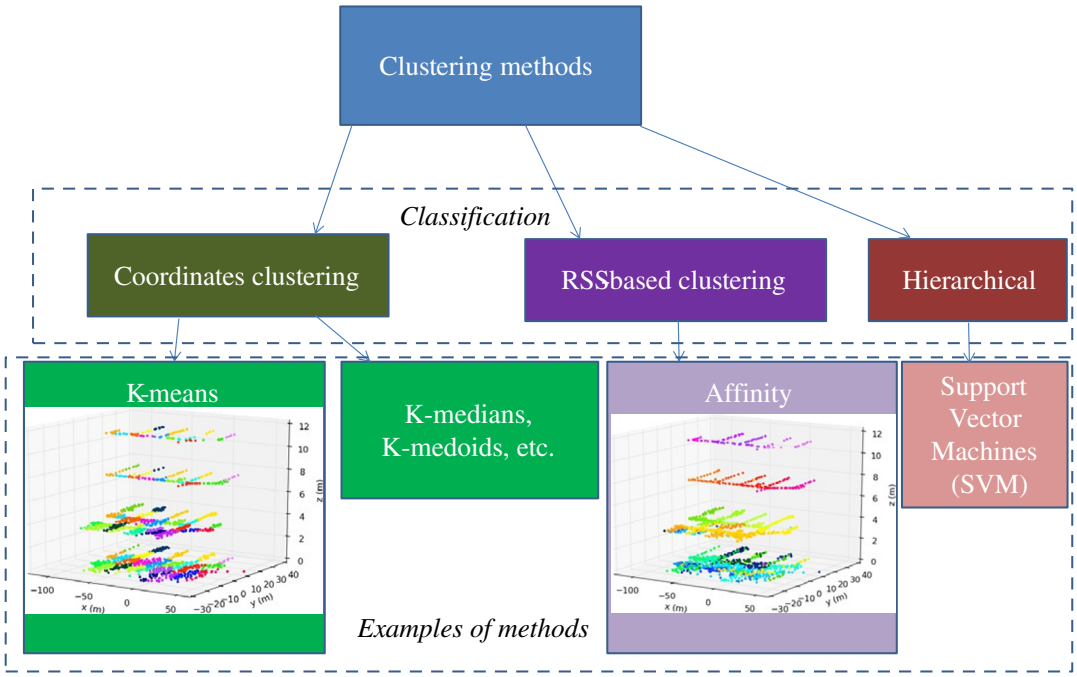

FIG. 2 Classification of clustering approaches with few examples.

the ath AP and the $\eta_{a,i}$ is a noise term, typically modeled via a Gaussian zero-mean process with variance σ_a^2, which incorporates the shadowing effects and the measurement errors. With this model, each AP is characterized by only three parameters: P_{T_a}, n_a, σ_a^2. Thus, instead of storing all the measurements at various training locations, with this PL approach it is enough to store these three parameters and the AP location x_{AP}, y_{AP}, z_{AP} per AP.

A major drawback with PL approaches is the additional inaccuracy created by the model misfit to the real data. More advanced PL models, for example, including floor losses and two-slope models, have been studied, for example, by Shrestha et al. (2013), where it was shown that the positioning error differences between the different PL models are very low, and that we usually loose between 20% and 30% in the positioning accuracy in PL models versus the full-training fingerprinting, but we gain up to 11 times in database reduction.

Multislope PL models have also been studied in Karttunen et al. (2016) and Munir et al. (2017), in a different context than wireless positioning. It is still an open research topic whether the multislope PL models can benefit the indoor wireless positioning and which PL models are best suitable for high-accuracy fingerprinting with reduced training database.

2.2.3 Image-Based Approaches

When considering global-scale positioning systems, one attractive approach for reducing the size of fingerprint databases is the spectral compression method presented in Talvitie et al. (2016). There, the fundamental idea has been to conduct the compression in frequency domain by applying an appropriate frequency transformation, such as Discrete Fourier Transform (DFT) or Discrete Cosine Transform (DCT).

In the spectral compression approach, the RSS values in the fingerprint database are processed individually for each network AP in the form of an RSS image, which represents a map of RSS values in a rectangular grid of geographical coordinates. Due to the fundamental characteristics of radio wave propagation, such as path-loss and shadowing effects, the nearby RSS values in the RSS image are correlated. Now, by considering the DFT, the Power Spectral Density (PSD) function of the RSS image can be defined as the DFT of the corresponding autocorrelation function.

Thus, based on the well-known time/frequency-scaling property of the Fourier transform, the PSD of the RSS image gets narrower, as the autocorrelation function gets wider. Physically, this means that the energy of the DFT-transformed RSS image is concentrated more tightly compared to the original RSS image. Moreover, the compression can be achieved by storing only the most significant frequency domain components which should include the majority of the useful energy of the original RSS image. However, since in practice some of the energy of the original RSS image is always left outside of the stored DFT coefficients, the described spectral compression approach is fundamentally a lossy compression technique.

It is convenient to represent the RSS image, that is, the observed RSS values for a single AP, as a matrix $\mathbf{G}_{\text{RSS}} \in \mathbb{R}^{M \times N}$, whose elements denote the RSS values (in dBm) in a rectangular grid. Furthermore, each column $n = 0, \ldots, N-1$ and each row $m = 0, \ldots, M-1$ determine a specific x-coordinate and y-coordinate for the corresponding RSS value. The total number of measurements is $N_m = N \times M$. Quite often some of the elements of $\mathbf{G}_{\text{RSS}}$ are missing, as there are no RSS measurements taken from those locations. Therefore, in order to complete the matrix, appropriate interpolation and extrapolation methods can be exploited as studied, for example, in Talvitie et al. (2015). In addition to interpolation and extrapolation methods, nonuniformly sampled frequency transformations are also feasible, but in these cases the computational complexity might grow unnecessarily large with respect to the gained advantage.

Typically the average observed RSS value of a RSS image, pointing out the zero-frequency element in the frequency domain, is significantly larger compared to the other frequency domain elements. As a result, the average RSS value would always be included in the compressed data, and therefore we can remove it from the RSS image and store it beforehand. By this way, a zero mean RSS image can be obtained as $\mathbf{G}^0_{\text{RSS}} = \mathbf{G}_{\text{RSS}} - \mu_{\mathbf{G}}$, where $\mu_{\mathbf{G}} = 1/(MN) \sum_{i=0}^{MN-1} \mathbf{G}_{\text{RSS}}(i)$, and where $\mathbf{G}_{\text{RSS}}(i)$ denotes the ith element of the RSS image matrix by using column-wise indexing. Now, in order to achieve the frequency domain representation without the need of using complex-valued quantities, a DCT is

employed in the following example. Consequently, the frequency transformed RSS image $\mathbf{H}_{\mathrm{RSS}}$ (of the same size with $\mathbf{G}_{\mathrm{RSS}}$) can be given as

$$\mathbf{H}_{\mathrm{RSS}}(k,l) = w_k w_l \sum_{m=0}^{M-1}\sum_{n=0}^{N-1} \mathbf{G}_{\mathrm{RSS}}^{(0)}(m,n)\cos\left(\frac{\pi\,(2m+1)\,k}{2M}\right)\cos\left(\frac{\pi\,(2n+1)\,l}{2N}\right), \text{ where}$$

$$w_k = \begin{cases} 1/\sqrt{M}, & k=0 \\ \sqrt{2/M}, & 1 \le k \le M \end{cases} \quad \text{and} \quad w_l = \begin{cases} 1/\sqrt{N}, & l=0, \\ \sqrt{2/N}, & 1 \le l \le N, \end{cases}$$

where $\mathbf{H}_{\mathrm{RSS}}(k,l)$ denotes the element of $\mathbf{H}_{\mathrm{RSS}}$ in the kth row and lth column. As show in Fig. 3, the energy of the frequency transformed image $\mathbf{H}_{\mathrm{RSS}}$ is heavily concentrated on one corner of the image. The original RSS image (on top of Fig. 3) is constructed based on linear interpolation and minimum method extrapolation, as given in Talvitie et al. (2015), by using the known RSS values in locations marked with ×. From the frequency-domain representation of the RSS image (on left), only the K largest energy components marked with ∘ are used to construct the compressed RSS image (on right).

Thus, by storing only the K largest elements from $\mathbf{H}_{\mathrm{RSS}}$ it is possible to generally reduce the amount of information required to represent the original image with adequate accuracy. It is not a straightforward task to choose an appropriate global value for the number of stored elements K, since the image size and the information content varies over separate APs. Hence, by considering each image separately, and choosing the K per image basis, will typically improve the performance of the compression process. Nonetheless, by assuming that the stored frequency domain elements are selected based on the order of element energy $|\mathbf{H}_{\mathrm{RSS}}(i)|^2$, the stored frequency components can be given as

$$\left\{\mathbf{H}_{\mathrm{RSS}}\left(q_s\right) \;:\; s = 0,\ldots,K-1\right\},$$

where q_s indicates the K elements with the highest energy. Besides the actual frequency component value $\mathbf{H}_{\mathrm{RSS}}(q_s)$, also the index q_s has to be stored into the database in order to recover the compressed RSS image. In addition, other parameters required to be saved are the image size parameters M and N, the physical image location, for example (latitude, longitude, altitude)-coordinate of one corner point, and the AP identity. It is worth noticing that the required bit resolution and the number of bits required to represent separate parameters might differ considerably, according to the environment. For instance, as the stored index values are concentrated on a single corner of the matrix, a reasonably designed entropy coder can easily achieve high compression ratios.

The reconstruction of the RSS images from the stored frequency domain components is rather straightforward. First, the compressed frequency domain image $\hat{\mathbf{H}}_{\mathrm{RSS}}$ is initialized with zero elements and the stored frequency domain components $\mathbf{H}_{\mathrm{RSS}}(q_s)$ are inserted in the corresponding element indices as

$$\hat{\mathbf{H}}_{\mathrm{RSS}}(q) = \begin{cases} \mathbf{H}_{\mathrm{RSS}}(q_s), & \text{when } q = q_s \\ 0, & \text{otherwise.} \end{cases}$$

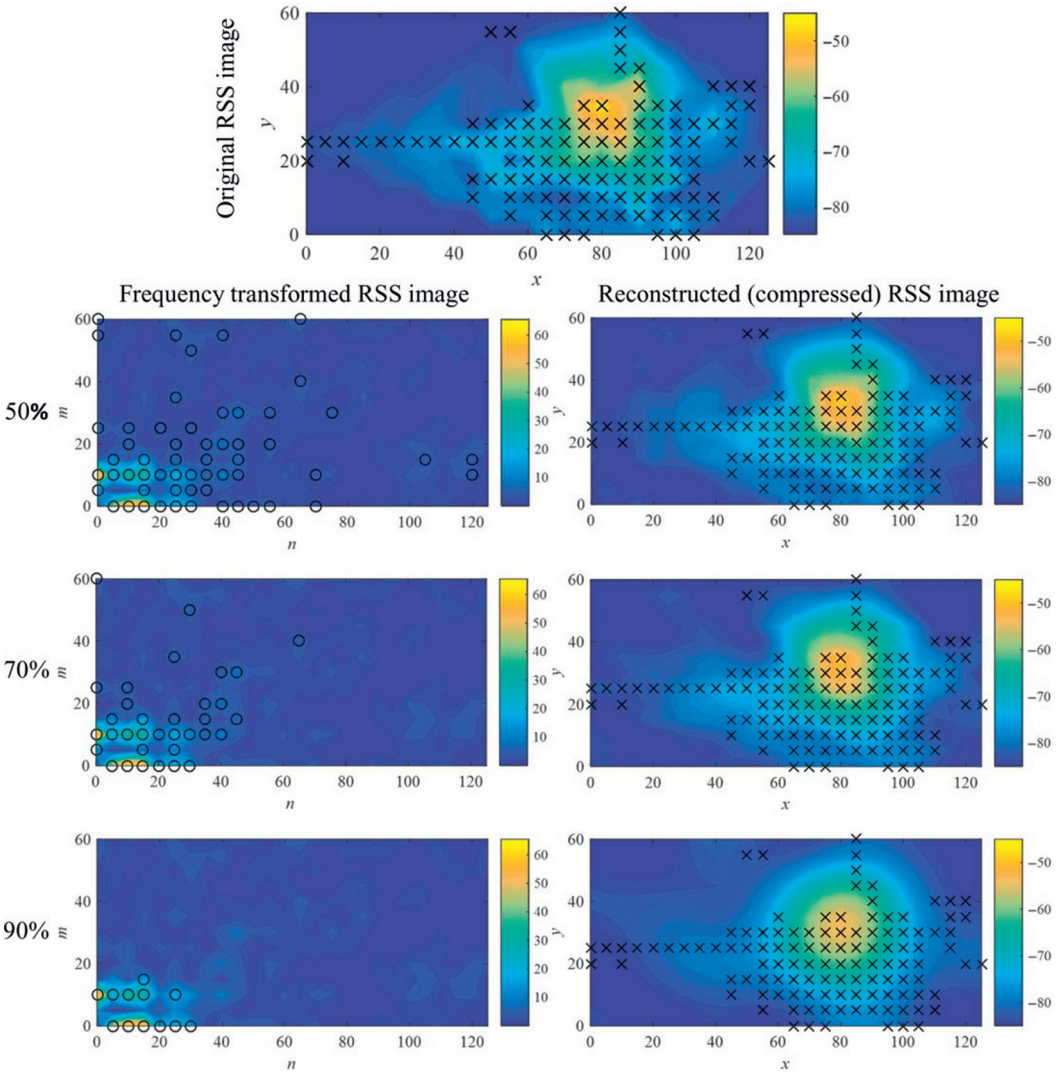

FIG. 3 Example of an image compression process with 50%, 70%, and 90% compression ratios. The original uncompressed RSS image (on the top) has been obtained by using the linear interpolation and minimum method extrapolation as given in Talvitie et al. (2015). The locations of the original RSS measurements used in the interpolation and extrapolation are marked with **x**.

After this, the compressed zero mean RSS image is obtained by taking the inverse frequency transformation, which in this case is the inverse DCT, given as

$$\hat{\mathbf{G}}^{(0)}_{\mathrm{RSS}}(m,n) = \sum_{k=0}^{M-1}\sum_{l=0}^{N-1} w_k w_l \hat{\mathbf{H}}_{\mathrm{RSS}}(k,l) \cos\left(\frac{\pi\,(2m+1)\,k}{2M}\right) \cos\left(\frac{\pi\,(2n+1)\,l}{2N}\right).$$

Finally, the compressed RSS image is obtained by adding the stored mean value as $\hat{\mathbf{G}}_{\text{RSS}} = \hat{\mathbf{G}}_{\text{RSS}}^{(0)} + \mu_{\mathbf{G}}$. In Fig. 3, the above described compression process has been illustrated for one indoor real-life RSS image of a WLAN AP, by using 50%, 70%, and 90% compression ratios.

In practice, when appropriately designed, the lossy nature of the spectral compression approach can actually benefit the positioning system. This is because of the built-in noise filtering property, in which during the compression, low energy spectral coefficients with poor signal-to-noise ratio (SNR) are automatically discarded from the database. It is worth noticing that by assuming uncorrelated noise between the RSS values in the original database, the noise energy spectrum is flat. Hence, the energy of the noise is distributed evenly on top of all elements of the frequency transformed RSS image.

One challenge is to find a good balance between the compression ratio and the noise filtering volume. A large compression ratio leads to good SNR of the database, but also to poor representation of the RSS data, and vice versa. Nonetheless, with appropriate parametrization, the positioning performance by using spectrally compressed database can reach, and even exceed, the performance of conventional fingerprinting with an uncompressed database. This has been illustrated by the results in Talvitie et al. (2016), as shown in Fig. 4, where the average positioning error has been provided by considering WLAN measurements over five separate buildings. Here, the positioning performance of the spectral compression is compared with the conventional fingerprinting and PL models as a function of compression ratio. It can be seen that the spectral compression can provide comparable performance with the fingerprinting method for compression ratios up to 70%–80%.

2.2.4 Other Approaches

A variety of other approaches have been proposed to deal with reduced-database fingerprinting, in various contexts, including wireless localization. For example, compressive sensing approaches (Milioris et al., 2011; Feng et al., 2012) take advantage of the inherent sparse structure of the RSS measurements inside a building, due to the fact that an AP is heard only in parts of a building. The feature extraction (Lin and Chen, 2016) or principal

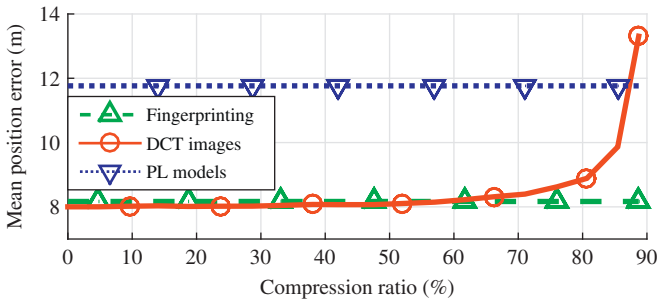

FIG. 4 The mean positioning error as a function of compression ratio of the spectral compression for conventional fingerprinting, path-loss models, and the RSS image approach.

component analysis (Mo et al., 2015) methods extract some relevant features from the set of the training data and use them in the estimation process. Multiclassifiers, extremely randomized trees and other machine learning approaches have also been studied, for example, in Uddin and Islam (2015) and Zou et al. (2016).

3 Challenges and Solutions in Fingerprinting

Table 2 summarizes the main challenges in RSS-based fingerprinting. Some of them have been already briefly addressed in the previous section, and some others are explained in more details below. Some others are only mentioned in this table with references for further reading. Table 2 also discusses different solutions to address these challenges and how some of these solutions support the objective of seamless positioning.

Several different phenomena can cause RSS fluctuations or an offset in the RSS values. Naturally, the positioning accuracy may decrease if the RSS in the database is clearly different than the RSS observed by the user in the estimation phase. RSS offsets can be divided roughly into constant, random, or localized bias (Laitinen, 2017). If an offset is caused by different equipment type, it is most typically modeled as a constant positive or negative bias. Temporal propagation dynamics such as user orientation or body losses in crowded periods during the training phase compared with the estimation phase can result in RSS fluctuations, i.e., random bias.

One of the main challenges in the two-phase localization methods is that the device used in the data collection process may be different than the device used in the estimation phase. As different devices with different chipsets scale the measured RSS values differently, the observed RSS at the same physical location may vary between different devices. According to Della Rosa et al. (2010a,b) and Kaemarungsi (2006), even 25–30 dB differences in RSSs for different devices have been noticed. In some cases the observed RSS values can be linear, as was noticed by Haeberlen et al. (2004) and Kjaergaard (2006), but due to chipset sensitivity, antenna spacings, antenna gains, and operating systems, linearity is not a guarantee (Della Rosa et al., 2010a; Wang and Wong, 2014). Fig. 5 illustrates the relation between RSS values in dB and the RSS indicator (RSSI) for three different chipsets (Atheros, Symbol, and Cisco). It can be seen that both the RSS scale and the steps differ between the chipset manufacturers remarkably.

Besides possible RSS offsets, another challenge in fingerprinting is the huge amount of data to deal with. Nowadays, the transmitter configuration can be very dense, meaning that the number of AP in an office building with several floors and plenty of offices is typically hundreds. High transmitter density naturally means that a lot of transmitters are heard in each measurement (i.e., in the training phase), leading into a huge amount of data to be handled. As also the number of fingerprints can be significant, the memory requirements for the database in large areas or with many buildings may become overwhelming, and data transmission may become a bottleneck for the positioning system, especially with fingerprinting.

Table 2 Overview of Challenges and Solutions in Fingerprinting

Challenge	Description	Possible Solutions and Seamless Support
Calibration issues	Difference or offsets in RSSs reported by different devices	Calibration methods.
Database sizes	Large training databases	Compressing the databases, e.g., spectral compression (Talvitie et al., 2016), AP reduction, sparse fingerprints, and interpolation.
Database gaps	Parts of the buildings are not accessible	Interpolation and extrapolation, e.g., in Talvitie et al. (2015) and Richter and Toledano-Ayala (2015). It may increase the positioning accuracy and the coverage area of the positioning system that integrates fingerprinting.
Height estimation	Height dimensions is often difficult to estimate accurately, especially in buildings with open spaces between floors	Use of 3D modeling and sensor aiding.
Channel modeling for single-stage methods	Finding adequate path-loss and shadowing models for the probabilistic approaches	Solutions found, e.g., in Shrestha et al. (2013), Karttunen et al. (2016), and Munir et al. (2017). May extend RSS-based seamless positioning to much larger areas.
Unknown location of emitters	For probabilistic approaches, knowledge of the AP location is typically important	Estimating the emitter location based on training data, e.g., as in Shrestha et al. (2013) and Varzandian et al. (2013).
Training data collection and updating	As wireless environments are highly dynamic, data need to be continuously collected, and updated or stored	Crowdsourced solutions, e.g., Chen and Wang (2015) and Wang et al. (2016) or automatization. Improves the accuracy of fingerprinting and, thus, the performance of the overall positioning system.
Server-mobile protocols and signaling	Location-related data needs to be transferred securely and robustly between server and mobile	Protocol design and secure communications solutions. Important for many positioning systems that rely on a client-server set-up. Standardized protocols facilitate the integration of those systems.
Low-cost positioning algorithms	This refers to the choice of the positioning signals, positioning algorithm, and data fusion approaches	Various studies can be found in Laitinen (2017), Kasebzadeh et al. (2014), and Liu et al. (2017), etc. Improved positioning and fusion algorithms improve the seamless positioning experience, e.g., Richter and Toledano-Ayala (2017).
Heterogeneity of training databases	Diversity of database structure, content and access to databases	Harmonization of fingerprint databases through, e.g., open (quasi) standards; hybridization with heterogeneous data. It facilitates the integration of different systems into one positioning system.

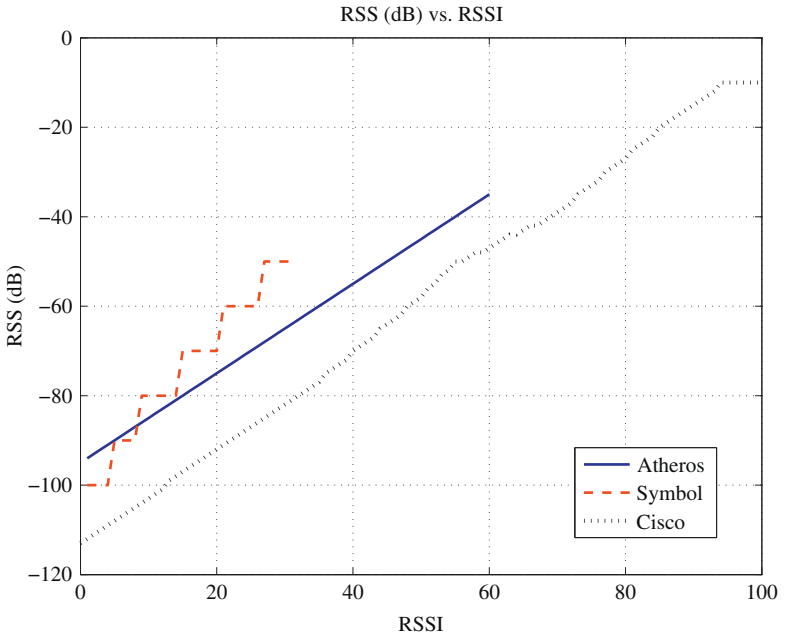

FIG. 5 The relation between RSS values in dB and RSSI for three different chipset manufacturers.

3.1 Calibration Issues

3.1.1 The Effect of RSS Offsets

RSS offsets and their impact on the positioning accuracy were studied, for example, in Chen et al. (2005), Vaupel et al. (2010), Laitinen et al. (2015), and Laitinen (2017). Chen et al. (2005) concentrated on the effect of three dynamic factors, namely relative humidity level, people presence and movements, and open/closed doors, on the positioning accuracy. Vaupel et al. (2010) studied the positioning performance of different devices in the same environment. More extensive research of the effect of an offset between the RSS values in the training and estimation phases for WLAN-based positioning was presented in Laitinen (2017) and Laitinen et al. (2015).

In Laitinen (2017), the effect of an offset between the RSS values in the training and estimation phases was studied by adding artificially a bias, b, to the original measured RSS. All results presented by Laitinen (2017) and Laitinen et al. (2015) are based on real RSS measurements in several multifloor buildings. Different offset types have been considered, and the bias can be chosen to be either a constant one, a random one or a localized constant bias, where a RSS offset occurs just for a certain part of the fingerprints.

Based on the research in Laitinen (2017), Fig. 6 presents two examples of the Cumulative Distribution Function (CDF) of absolute distance error for two different measurement set-ups, for different bias types. For constant biases, the artificial bias is chosen to be $b = \pm 10$ dB, $b = \pm 20$ dB, and $b = \pm 30$ dB. In the case of random bias, the amount of a bias

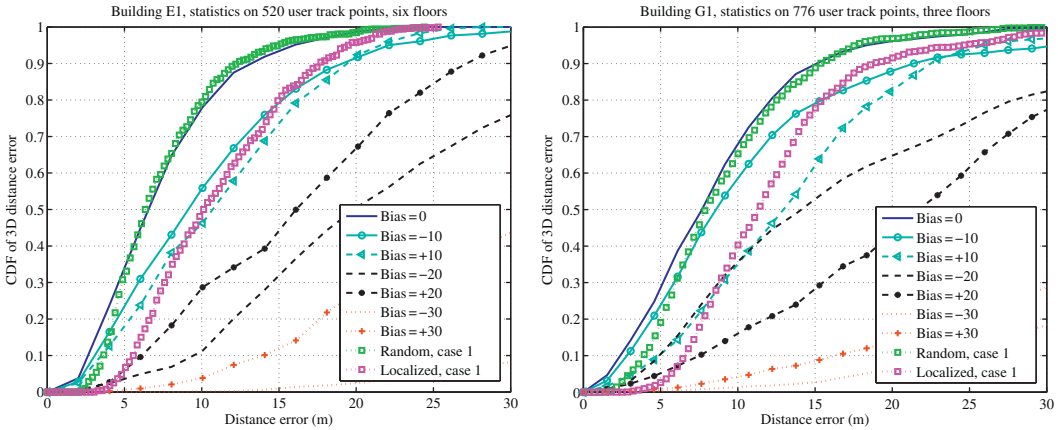

FIG. 6 CDF of absolute distance error for two measurement set-ups: six-floor shopping mall *(left)* and three-floor shopping mall *(right)*.

is varied randomly between −10 dB and +10 dB according to uniform distribution. In the case of localized bias, −10 dB artificial bias is set up for 50% of the FPs in the database, and +10 dB bias for the remaining 50% of the FPs.

As seen in Fig. 6, a random bias between −10 dB and +10 dB affects the results very little. Thus, small RSS fluctuations can be easily neglected. Constant RSS offsets, including the localized case, clearly affect more. A negative constant bias of −10 dB increases the mean distance error less than 20% in general, whereas a positive constant bias of +10 dB is more severe, it increases the averaged mean distance error more than 50% (Laitinen, 2017; Laitinen et al., 2015).

3.1.2 Possible Calibration Methods

If the RSS offset between different equipments is wide, some calibration is needed in order to compensate the possible deterioration in the positioning accuracy. Various calibration techniques have been studied in the literature, for example, Haeberlen et al. (2004), Vaupel et al. (2010), Machaj et al. (2011), Kjaergaard (2006), Kjaergaard and Munk (2008), Cheng et al. (2013), and Wang and Wong (2014). Calibration methods can be performed in offline (training) or online (estimation) phase. Offline calibration means premapping between different equipment in the training phase. It requires a lot of measurements and large datasets in order to be able to calculate models for appropriate mapping. If the dataset is collected with one device only, it is also possible to use so-called learning period before the localization phase with another device (Haeberlen et al., 2004; Kjaergaard, 2006). In online calibration, no mapping models are needed, but the adaptation is obtained using, for example, RSS differences (Hossain et al., 2013) or RSS ratios (Kjaergaard and Munk, 2008; Cheng et al., 2013) instead of absolute RSS values in the training database.

The smallest enclosing circle-based fingerprint clustering from Liu et al. (2016) is another method proved to help in calibration and to improve the position accuracy

up to 29%. An interesting alternative to online adaptation is to use so-called test rank based method proposed in Machaj et al. (2011), where the detected transmitters in the measurement are sorted according to their RSS values. The order of the transmitters forms the so-called ranking vector, and in the positioning phase, only these ranking vectors of the FP and the mobile are compared. A similar approach is also presented in Yedavalli et al. (2005). However, also these approaches, assume that the order of the sorted RSS values is the same between different devices. More discussion on different calibration schemes can be found in Jung et al. (2017), for example.

3.2 Database-Size Reduction

Another challenge in fingerprinting is when we deal with mobile-centric positioning and need to transfer a large amount of data from the location server side to the mobile side in order to enable the mobile device to compute its own position. In such situations, it is important to reduce the size of the databases transferred from the server side to the mobile side, not only to increase the speed of the position computation, but also to lower the mobile's battery consumption and to decrease the data consumption at the mobile side. Some of the methods to achieve a reduction in the training databases transferred to the mobile are discussed in the following subsections.

An obvious way to reduce the amount of transmitted data is to decrease the number of fingerprints. Increasing the average distance between fingerprint locations of the training database is one option to achieve that, for example, by increasing the fingerprint grid size and average the neighboring RSS, by simply subsample the fingerprints, or by collecting the fingerprints sparsely, in the first place, and then interpolate RSS spatially. Naturally, there is a trade-off between the positioning accuracy and the density of fingerprints.

3.2.1 Compression and Clustering

Compression and clustering methods for training databases are a further option to decrease the amount of data to be transmitted from the network or location server to the mobile side. At this point, the reader is referred to the discussion in Section 2.

3.2.2 Access Point Number Reduction

The primary target for the WLAN network configuration is to guarantee a good coverage and to serve plenty of simultaneous users as efficiently as possible. The AP infrastructure may therefore include several transmitters located very close to each others, or transmitters that are part of a virtual WLAN, using multiple MAC addresses and Basic Service Set Identifiers (BSSID), which will be seen as several transmitters at the same location. From a positioning point of view, the data transmitted by those APs is likely to be highly correlated and therefore redundant. Thus, not all of the heard APs add information to the positioning, that is, the position accuracy is retained if that information were removed. This data only increases the storage demands and the complexity of the localization process unnecessarily and a reduction is commonly desired.

AP selection has been widely studied (Fang and Lin, 2012; Zou et al., 2015; Zhou et al., 2013; Miao et al., 2014; Liang et al., 2015; Youssef et al., 2003; Chen et al., 2006; Kushki et al., 2007). In addition, AP selection together with the grid interval and with several positioning approaches has been addressed in Laitinen (2017) and Laitinen and Lohan (2016). AP selection can be done in the online positioning phase (Kushki et al., 2007; Zou et al., 2015), in the offline training phase (Youssef et al., 2003; Chen et al., 2006; Zhou et al., 2013), or by taking into account both phases (Laitinen et al., 2012; Miao et al., 2014). However, the biggest advantages are achieved when the selection is performed already in the training or offline phase, in order to reduce the amount of stored and transferred data.

The most used AP selection methods are max-mean proposed in Youssef et al. (2003) and InfoGain (also called Entropy) proposed in Chen et al. (2006). The best selection criteria for both fingerprinting and path-loss-based positioning approaches was shown in Laitinen (2017) to be the maxRSS criterion, where 40% or more of the available APs are chosen to form the AP subset, based on the RSS values sorted from maximum to minimum. Another interesting criterion is called multiple BSSID selection, where the idea is to choose only one AP among the closely located ones (i.e., within one meter), in order to remove the correlated data (Laitinen, 2017). According to Laitinen (2017) and Laitinen and Lohan (2016), up to 60% of the APs can be removed without deteriorating significantly the localization performance. However, with this criterion, the number of closely located AP or those supporting multiple BSSID is dependent on the building, and therefore the percentage of removed APs may vary between only few percent and up to 60%. Thus the gain in the database reduction can be smaller than in the case when maxRSS selection criterion is used.

3.3 Measurement Gaps

For a global localization system, it is extremely challenging to achieve a complete fingerprint measurement set with no geographical measurement gaps. Even if one invested in particularly extensive measurement campaigns, there would always be areas with restricted access, which basically would decline the opportunity for achieving full coverage databases. In addition, maintaining and updating a global fingerprint database are enormous tasks, which can by themselves lead to coverage gaps. For instance, this could happen when the measurement data from specific area is declared outdated before new measurements become available.

In order to mitigate the negative effects of the coverage gaps, the missing fingerprints need to be estimated. This is fundamentally an interpolation and/or extrapolation task. In this context, the term interpolation refers to the process where RSS values are estimated for measurement gaps between available fingerprint coordinates, that is, inside the convex hull of the fingerprint coordinates. Moreover, the term extrapolation refers to the estimation of RSS values outside the convex hull of the fingerprint coordinates. From these two, the extrapolation task is usually more challenging than the interpolation task due to the poor geometry of the known RSS values and large average distances to the closest known RSS values. In addition, whereas with conventional interpolation techniques the RSS

estimates are naturally limited by the known neighboring RSS values, many extrapolation techniques, such as gradient-based extrapolation, might produce RSS estimates which are out of the range from sensible physical values.

When considering a target area with precollected fingerprints, the actual total number of fingerprints is not necessarily the most important parameter, but more likely the distribution of the fingerprint coordinates is the crucial information. Hence, missing a fingerprint here and there does not affect as much as missing a large chunk of fingerprints from a certain location. However, due to the complicated nature of the positioning system, which is highly dependent on the considered environment, it is challenging to approximate how the possible coverage gaps in the database affect the system performance when compared to full coverage database. In addition, it is as interesting to find out how the above-mentioned interpolation and extrapolation techniques can facilitate the mitigation of negative effects caused by the coverage gaps.

One approach in order to study the effect of coverage gaps on the system performance is to first collect a solid set of fingerprints from the target area, and then, to artificially remove fingerprints from the dataset. Now, by comparing the performance between the original full coverage dataset and the dataset with removed fingerprints, the effects of missing fingerprints should become evident. However, as stated before, it should be noticed that removing arbitrary fingerprints here and there does not reflect the case of realistic coverage gaps in the database. As studied in Talvitie et al. (2015); Talvitie et al. (2014), one way to mimic realistic coverage gaps is to remove fingerprints in specific areas, where all fingerprints within a certain distance from a randomly selected location, are removed from the database. Then, after removing the desired number of fingerprint chunks, the resulted database can be used for studying the positioning performance.

An outcome of an arbitrary fingerprint removal process for a database with indoor WLAN measurements is illustrated in Fig. 7, where the original database is compared with the databases from which 30% of the data points have been artificially removed. In the other set, the data points have been removed uniformly, and in the other, the removal process has been done based on the fingerprint chunks. From here it is evident that the chunk-based removal method introduces more substantial coverage gaps in the database compared to the uniform removal. The radius of the fingerprint chunk can be determined based on the physical dimensions of the studied positioning environment, for example, based on the average room size for indoor scenarios, or on the average block size in a street plan for outdoor city environments.

The effect of coverage gaps on the positioning accuracy has been presented in Talvitie et al. (2015), where an indoor database consisting of WLAN APs in a large university building is studied over different database coverage gap scenarios.

In Fig. 8, the effect of coverage gaps on the positioning accuracy is compared between the original database, the databases with coverage gaps, and the databases where the coverage gaps have been filled by interpolation and extrapolation. In this case, the interpolation and extrapolation has been performed based on Inverse Distance Weighting (IDW) method, where an RSS estimate for any location (x, y) is obtained as a weighted average over the known RSS values as

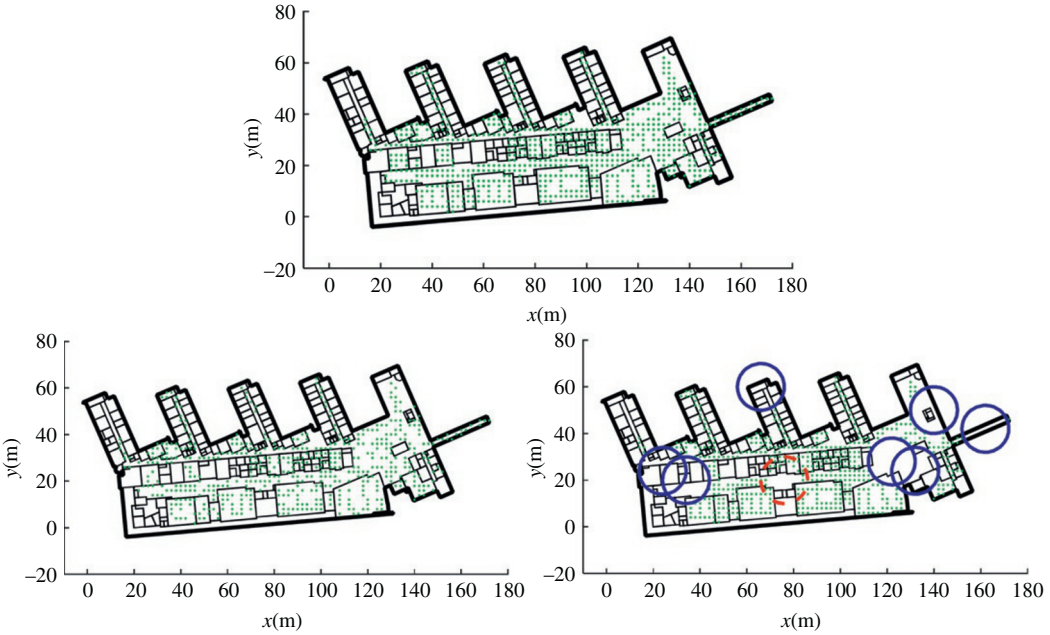

FIG. 7 Example of original fingerprint database (on *top*), and the corresponding databases after randomly removing 30% of the data points, based on uniform removal (on *left*) and chunk-based removal (on *right*). The *continuous circles* indicate the locations of the removed chunks, and the *dashed circle* is the last removed area, where part of the fingerprints has been retrieved in order to achieve the exact desired database reduction percent.

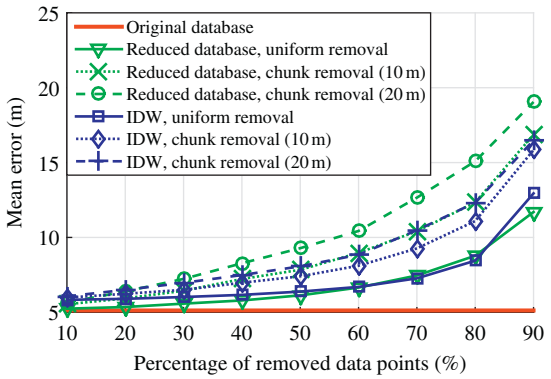

FIG. 8 Mean positioning error as a function of data point removal percentage for the original database and the reduced databases, including both the uniform removal approach and the chunk removal approach (with 10 m and 20 m chunk radii), and for the IDW-based interpolated/extrapolated database.

$$\hat{P}_{\mathrm{RSS}}(x,y)=\sum_{i=0}^{L-1} w_i P_i(x_i,y_i), \quad \text{with} \quad w_i=\frac{d_i^{-u}}{\sum_{j=0}^{L-1} d_j^{-u}} \quad \text{and} \quad d_i=\sqrt{(x_i-x)^2+(y_i-y)^2},$$

where w_i and $P_i(x_i, y_i)$ are the ith weight and the corresponding known RSS value at location (x, y). The AP subscript has been dropped here for clarity, as such approaches are applied for each AP. Moreover, d_i is the distance between the estimate location and the location of the ith known RSS value, and L is the number of known RSS values in total. Fig. 8 shows that when the number of coverage gaps increases, that is, the number of fingerprints in the database is reduced, the performance offered by the interpolation/extrapolation improves. In addition, it can be observed that the performance degradation caused by uniformly removed fingerprints is at considerably lower level compared with the chunk-based removal process.

3.4 Height or Floor Estimation

A further challenge in indoor fingerprinting is encountered in multifloor buildings with open spaces, such as malls or automation halls. The floor identification or the exact height estimation in such scenarios is very challenging. There are two ways of looking at this issue: On one hand, the fingerprints can be collected and stored per floor, with a floor index $f = 1, 2, \ldots$ saved as the height dimension, no matter of the height of the measurement device used to collect the measurements. On the other hand, the exact height of the fingerprint can be inferred from additional sensor measurements such as barometer or accelerometer readings, then the z-coordinate would reflect the mobile's height. At the present time, there are very few articles investigating which of these two approaches is better. For example, Xiao et al. (2017) shows that vertical accuracy can be improved with a 3D model where the fingerprints height is perfectly known. Floor detection studies can also be found in Jia et al. (2016), Moreira et al. (2016), and Razavi et al. (2015).

4 Integration of WLAN With Other Signals of Opportunity

While there are already solutions capable of achieving submeter level performance in some indoor environments (Kotaru et al., 2015), not a single system can be seen as the ultimate solution for indoor scenarios or for seamless positioning. Especially one that can accommodate cost, battery performance, and different degrees of positioning accuracy (Liu et al., 2007).

The plenitude of man-made and natural signals offer a significant advantage indoors compared to outdoor scenarios, where cellular network and satellite signals are often more predominant. Hence, in indoor scenarios there are many man-made signals, from different spectra such as radio and light, or sound, and with their own very specific purposes. For example, WLAN (or WiFi) networks have the purpose of exchanging data between network peers, visible light installations aim to illuminate the building areas, while others, such as pressure and magnetic fields, are a naturally occurrence due to our planet's inner workings.

However, all of these have their own characteristics and traits which can be exploited for other purposes, including positioning. This section aims to cover the use of some of these sources, called signals of opportunity—signals not originally created with the positioning purpose in mind—and their combination to tackle the problem of indoor positioning.

4.1 Signals of Opportunity and Their Characteristics

As mentioned before, a signal of opportunity (SoO) is any wireless signal which can be used for positioning purpose, but which has been designed with other objective in mind, such as communication, or illumination, etc. When it comes to identifying signals of opportunity, the main goal is to build on existing systems and their own characteristics (Coluccia et al., 2014). In indoor scenarios, WLAN networks have become one of the prime systems that have been exploited for positioning purposes, especially due to their ubiquitousness and integration with mostly all mobile devices. In addition to WLAN, several Bluetooth-complaint technologies are making their way into the majority of user electronics. Nowadays, BLE, for example, is widely encountered on many wireless mobile devices. RFID is another technology that provides SoO and which is more and more used in various applications such as logistics, inventory tracking, conference attendee tracking, or interactive management.

Considering ubiquitousness of a technology provides a good way to identify a SoO. A second concern is the exploitation of the most appropriate system characteristic. In this regard, one has to take into account the principle of operation of such systems and look for specific parameters, such as clock accuracy, channel bandwidth, signal modulation, propagation, among others. In addition to these, one also has to take into account how to aggregate and process these measurements in order to provide a position solution.

With this in mind, Table 3 provides a qualitative overview on certain SoO measurements and their advantages and disadvantages. The measurements in the time and angle domain typically require dedicated hardware. For that reason, RSS is one of the most interesting feature to build upon for an opportunistic positioning.

Table 3 A Qualitative View Regarding Derivatives From Potential Signals of Opportunity

Measurement	Advantages	Disadvantages
Received Signal Strength	Inherent characteristic	Hardware dependency
	Low cost and burden	Sensitive to multipath
Time of Arrival	Lax clock requirements for the network	Requires precise clock in the device
		Sensitive to small clock errors
		Usually requires estimation of time component
Time Difference of Arrival	Lax clock requirements for the device	Requires precise clock in the network
Angle of Arrival	Builds on signal's phase	Requires antenna arrays or specialized antennas
		Accuracy decreases with distance to target

Thus, the next two sections offer two case studies on the combination of RSS from several systems, such as WLAN, BLE, and RFID. While not the focus of our study, geomagnetic fields can also be used as a signal of opportunity as pointed out in Pasku et al. (2017), Shu et al. (2015), and Zhang et al. (2015).

4.2 WLAN and BLE

This section highlights the use of WLAN and standard BLE RSS measurements. This case study uses data from two measurement campaigns carried at the Tampere University of Technology.

BLE has risen in popularity over the last years, especially as a connectivity standard for smaller gadgets, such as smart watches and TVs (DeCuir, 2014). However, its low power has also enabled several location-based services, through the use of its beacon functionality. In such mode, the devices advertise, at a time, in one of three advertisement channels. As such advertisement is caught by scanning devices, such as mobile phones or other dedicated hardware, the RSS indicates the proximity to such tag. Hence, this system is finding its way in the indoor positioning market, where it is often used as an advertisement means to push people into buying a specific product.

The predominance of both BLE and WLAN signals in indoor environments make them an interesting subject of study, allowing one to delve into the benefits of combining RSS measurements from such systems. Hence, this study combines data from two separate measurement campaigns, each used to capture either WLAN or BLE signals, by merging them in postprocessing. Merging these datasets is possible as both datasets are georeferenced in the same local frame.

Overall, our case study shows a small increase in accuracy when combining both technologies, as shown in Fig. 9. In terms of RMSE the combination of both technologies leads to 6.07 m versus, 7.81 m for BLE and 6.71 m for WLAN. While there is an improvement in accuracy when merging both technology, it is not significantly higher than the WLAN-only positioning. One might conclude that the reasons behind this are twofold: on one hand, both technologies operate in the same frequency band, which leads to similar propagation conditions for both technologies, and thus to correlated measurements, and on the other hand, as the WLAN network in the studied building is very dense (more than 500 unique SSIDs within four floors and a horizontal area of about 150 $m \times 100\ m$), adding additional BLE transmitters brings in little additional benefit. An open question here is how such a WLAN-BLE fusion would behave in buildings with very low density of APs.

4.3 WLAN and RFID

In this section, we present a case study of combined WLAN and RFID measurements as the inputs for a fingerprinting algorithm with full training database. This study is based on simulations of RSS in WLAN and RFID, followed by field experiments conducted in several studies (especially Hasani et al., 2015 and Lohan et al., 2014) at the Tampere University of Technology.

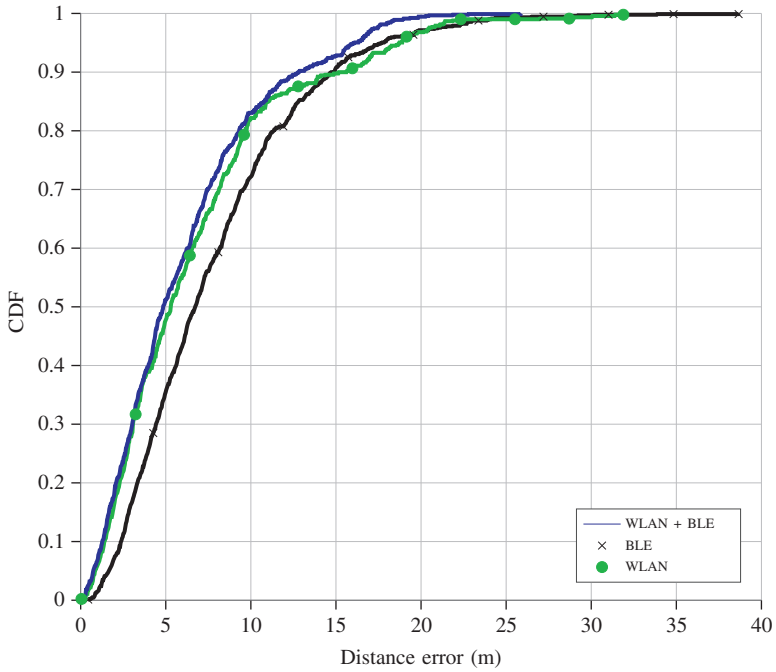

FIG. 9 Positioning performance with WLAN, BLE, and both technologies combined.

RFID has been a leading solution in the field of security for many years and seen as a contender to solve the indoor positioning dilemma. While the cost of its tags is rather negligible, its infrastructure costs is demanding, not only monetarily, but also power consumption wise. Nevertheless, despite its shortcomings, it is a feasible contender in the indoor positioning challenge. The goal of this study was to investigate the benefits that RFID could bring when matched together with WLAN.

In the case study shown here, we made the assumption that four RFID readers were placed in the center of a 25 by 25 m area in two distinct environments: (i) one where WLAN signals are highly available and (ii) another where WLAN signals are scarce. In more detail, for such environments, we assume approximately four APs per 100 m^2 (high availability) and about two APs per 100 m^2. The results are shown in Fig. 10A and B.

Fig. 10 shows first a benefit in both cases of a combined approach compared with the RFID-only and the WLAN-only approaches. Second, it can be seen that the gain in low density WLAN environments is much higher than in a high density WLAN environment, as intuitively expected. In Fig. 10B, the performance gain of the joint positioning is approximately 20% at 4 m error compared with the single-system positioning.

Finally, the figures also point out that position estimates based on RFID are only achievable 40% of the times. This means that the remaining 60% of times, a position estimate is unavailable as the signal strength is below the receiver sensitivity. In other words, the short range of RFID is a liability for a positioning system focused solely on this technology.

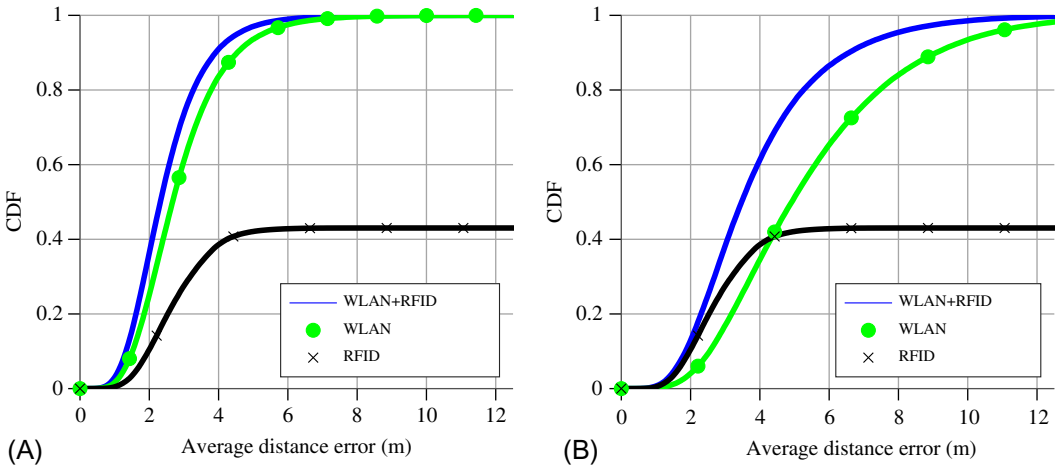

FIG. 10 Positioning performance with WLAN, RFID, and both technologies combined in a simulated scenario. (A) High availability of WLAN; (B) Low availability of WLAN.

5 Integration of WLAN With GNSS

As pointed out in the previous sections, a positioning system that provides seamless accurate location information in indoor and outdoor environments is still lacking. An open issue is particularly the position accuracy in environments that are not indoors, but where GNSS positioning is heavily degraded due to the lack of line-of-sight (LOS) to the satellites. Examples for such environments are the transition zones between indoors and outdoors, semiopen spaces with light or only partial roofs, and also densely constructed city centers.

A common strategy to provide accurate positioning in these areas is to combine GNSS with indoor location systems, such as WLAN-based positioning. The range of WLAN signals and their ability to penetrate structures enable seamless positioning. This section focuses on solutions to seamless indoor/outdoor positioning by merging GNSS and WLAN.

Several different approaches for the integration of GNSS-based positioning and WLAN-based positioning have been published. Depending on their level of integration or type of measurement they can be categorized in three groups:

1. methods that *switch* between GNSS and WLAN derived position estimates,
2. methods that *average* the position estimates from both systems, and
3. methods that *fuse* information from each of the systems and then compute a joint position estimate.

Most of the systems that belong to the first category simply use the availability of GNSS to choose which system to use. Another criterion to decide for one or the other system

is the energy consumption, or an additionally derived accuracy measure for the position estimate of the subsystems.

Methods of the second category combine the position estimates from GNSS and WLAN by either computing the weighted average, or by sequential Bayesian filtering. To perform reliably, these approaches need to determine adequate weights (in a Kalman filter, e.g., the weights are determined by the measurement covariance); this is crucial and usually the biggest challenge.

The third category of approaches yields a position estimate by fusing GNSS pseudoranges with either ranges or RSS deduced from WLAN signals. Such methods can be used even when less than four satellites are in view. RSS from just a few AP can be beneficial, so that the robustness compared with the stand-alone solutions is improved, together with accuracy and precision.

In particular the methods that belong to the latter group, that integrate raw-data to a common solution, are able to yield accurate seamless positioning and are therefore detailed in the following subsections. For further information about the other approaches we refer to Richter et al. (2014) and the references therein.

5.1 Fusing GNSS Pseudoranges With WLAN Ranges

The integration of GNSS pseudoranges and WLAN ranges is conceptually straightforward. GNSS pseudoranges and WLAN ranges are joined in a common set of multilateration equations which can be solved by a least-squares method or a closed form solution such as Bancroft's algorithm. The works by Li and O'Keefe (2013) and Nur et al. (2013) are notable advances in that topic. They also showed that, based on the current hardware, timing, synchronization, and NLOS condition still pose a challenge for ranging with WLAN signals. The LOS requirement is especially hard to fulfill and hinders these approaches in achieving accurate seamless positioning. WLAN hardware supporting the Fine Timing Measurement procedure and eventually the new generation WLAN standard (IEEE 802.11az) are expected to push the accuracy of these fusion approaches further.

5.2 Fusing GNSS Pseudoranges With WLAN RSS

Fusing GNSS pseudoranges and WLAN RSS means to combine different physical quantities. This is achieved by encoding the information of the different measurements in a universal manner. The existing approaches (Hejc et al., 2014; Richter and Toledano-Ayala, 2017) compute a joint likelihood function from the observed pseudoranges and RSS. To obtain a position estimate from the joint likelihood function one may compute the maximum likelihood estimate. The Bayesian point estimates are also a common choice.

Due to the use of fingerprinting on the WLAN side, the overall system shares the challenges of fingerprinting methods, most prominently, those referring to the construction and maintenance of the training database. An additional issue when it comes to fusing pseudoranges and RSS are the different state spaces. The state space of pseudoranges

is continuous, whereas the fingerprints are defined on a spatially discrete state space. Recently, Gaussian process (GP) regression, a machine learning technique, was proposed to alleviate both issues (Richter and Toledano-Ayala, 2017).

Gaussian processes (Rasmussen and Williams, 2006) are a generalization of multivariate normal distributions: instead of a mean vector and a covariance matrix, they are specified by a mean and covariance function. In the context of WLAN fingerprinting, the Gaussian processes exploit the spatial correlation of the RSS samples (fingerprints) to establish a model that permits to regress RSS spatially. Gaussian process regression is also known as "kriging." After the model is learned, fitted to the RSS fingerprints of the training database, RSS can be interpolated at arbitrary positions. The effort of constructing the radio map is alleviated, because fewer fingerprints are required to achieve comparable localization performance as using dense fingerprints and no interpolation (Schwaighofer et al., 2004). The different state spaces are addressed, because the Gaussian process model provides a continuous functional representation of the spatial RSS distribution.

The method reported in Richter and Toledano-Ayala (2017) is illustrated in Fig. 11. It inherits the training and estimation stage from fingerprinting and incorporates Gaussian process regression in a particle filter (PF) in the estimation stage.

5.2.1 Training Stage

During the training stage, or offline phase, the algorithm proposed by Richter and Toledano-Ayala (2017) creates the radio map and computes a Gaussian process model for each access point. To find an appropriate Gaussian process model for one access point a mean and a covariance function has to be specified a priori. In a second step the parameters of these functions, so called hyperparameters, have to be found by fitting the

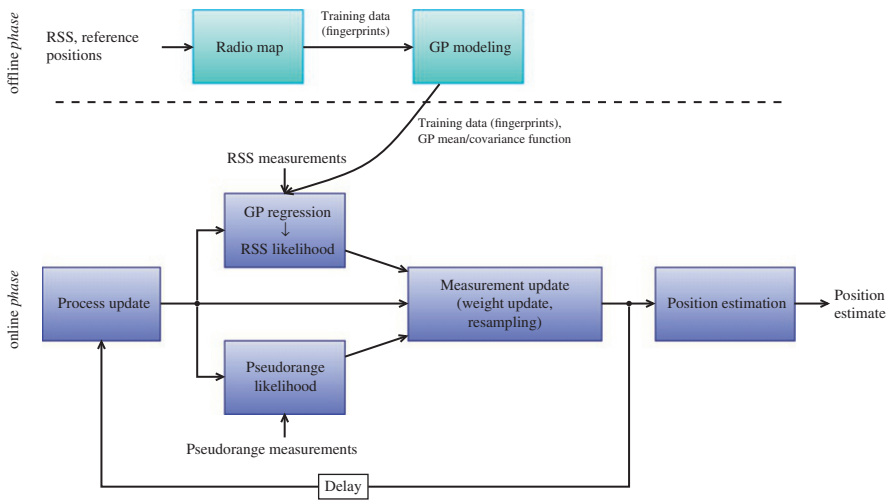

FIG. 11 Flow chart hybrid positioning system based on Bayesian filter fusing GPS pseudoranges and WLAN RSS.

mean and covariance function to the fingerprints (They define the mean and covariance functions' specific form.). Once the model is trained, that is, the optimal hyperparameters for the chosen mean and covariance function are found, the resulting Gaussian process model provides a continuous functional description of RSS over space. Such a model has to be obtained for each access point.

From the mean function of the trained Gaussian process RSSs can be predicted, and the covariance function gives corresponding variance estimates for these RSSs. The variance stems from the spatial correlation captured in the model. The correlation between neighboring RSS declines the larger their distant. Predicted RSS farther away from fingerprints have larger variance and, thus, areas lacking training data have larger variance than areas in which fingerprints are available.

5.2.2 Estimation Stage

In the estimation stage, or online phase, Richter and Toledano-Ayala (2017)'s algorithm employs a generic particle filter (Ristic et al., 2004) to track the mobile. A particle filter approximates numerically the recursive Bayesian estimator consisting of the process update and the measurement update. The process update models the motion of the mobile. The outcome of the process update is a distribution that predicts the position of the mobile at the next time step based on the current position and using the motion model. In Richter and Toledano-Ayala (2017) a random walk velocity process is used as process model.

The measurement update corrects the predictions made before in the process update. This correction incorporates the information of the measurements in form of a likelihood function and provides the posterior distribution. For each set of observables—a set of pseudoranges, one for each satellite, and a set of RSSs (averages), one for each access point—a likelihood function is required. Richter and Toledano-Ayala (2017) model both, pseudoranges and RSS, as normally distributed random variables.

The pseudoranges are modeled as sum of the geometric distance between receiver and satellite, plus the clock offset and normally distributed noise. A variance for each pseudorange is estimated by the GPS receiver and is based on the User Range Accuracy.

To model the RSS average, the Gaussian process model from the training stage is used. The noise is again assumed to be normally distributed and a Gaussian likelihood function is established. Its mean and variance are computed by using the mean and covariance function of the Gaussian process model.

The key idea of particle filtering is to sample the functions involved in the process and measurement update of the Bayesian filter, so that integrals are replaced by sums which then can be solved numerically. During one cycle of the recursion (see online phase in Fig. 11) the process update predicts the mobile's location based on the motion model and a previous estimate of the location, and the measurement update corrects this prediction by incorporating the observations in form of the mentioned likelihood functions. The outcome of the measurement update is the posterior distribution of the mobile's location.

This posterior distribution describes the location estimate and its uncertainty and is also input for the following cycle. A position estimate can simply be the maximum of the posterior distribution or the conditional mean.

Noteworthy is the choice of the variances in Richter and Toledano-Ayala (2017). In the case of pseudoranges they are obtained from the GPS receiver at each epoch. The variance of a RSS observation is provided by the Gaussian process model, thus, encodes spatial information instead of temporal information.

5.2.3 Performance of Pseudorange and RSS Fusion Filter

The performance of the above presented fusion scheme has been investigated in an indoor/outdoor environment harsh for GNSS and WLAN fingerprinting (Richter and Toledano-Ayala, 2017): Large parts of the test tracks are on semiopen, roofed passageways along the buildings, several trees cover the open area of the testbed; moreover, fingerprints have been established not only on the tracks, but as well on the open spaces between the buildings. Thus, this test environment is rich in multipath and ambiguous fingerprints and presents a typical case for seamless positioning.

The positioning results for two test tracks (Track-1 and Track-2) of the proposed PF are compared with that of an extended Kalman filter (EKF). Both filter employ the same process update. The EKF processes pseudoranges, as typical in GNSS receivers, and integrates a position estimate from the fingerprinting-based system.

The general performance of this approach to seamless positioning is depicted in Fig. 12. Track-1 has more indoor sections, it starts in the left building and enters the right building toward the end of the path (cf. solid path with arrows). Track-2 consists of more outdoor sections as it starts outdoors on the large open space, takes a rectangular path on the lawn area toward the right building. The track's only indoor section is in the northern part of the right building, from where it continues to the left building, where it circles the small lawn

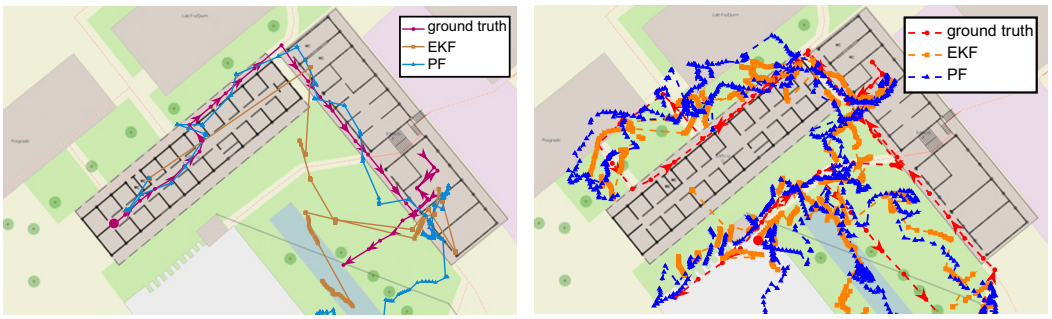

FIG. 12 Testbed, ground truth, and estimates of Track-1 and Track-2 of seamless indoor/outdoor positioning experiment using GPS pseudoranges and WLAN signal strength. (A) Track-1; (B) Track-2 (© OpenStreetMap contributors).

area between the buildings and then returns to the large open space area where it started (cf. red, solid path with arrows).

The PF's estimates of Track-1 (cyan, triangle, solid) follow the ground truth quite well. Larger deviations can be observed in the last third of the track in the indoor part of the right building and in the following outdoor section. The EKF performance on that track (magenta, square, solid) is rather poor. For Track-2, both filter perform similarly. Both filter estimate well the indoor section. During the section outside of the left building the accuracy of the EKF appears higher than that of the PF.

The empirical cumulative distribution function of the two filters is shown in Fig. 13. The PF has a median accuracy of 5 m for both tracks, whereas the EKF yields about 10 m for Track-1 and 6 m for Track-2. Excluding for a moment the EKF for Track-1, the error for fusing pseudoranges with RSS is below 10 m in 90% of time. The large maximum error of the PF for Track-2 is due to the poor initial estimate.

Table 4 summarizes the above results in terms of the mean absolute error (MAE). It compares additionally the PF hybrid solution with particle filter configurations in which either only GPS or only WLAN is used. The combination of both sources of information

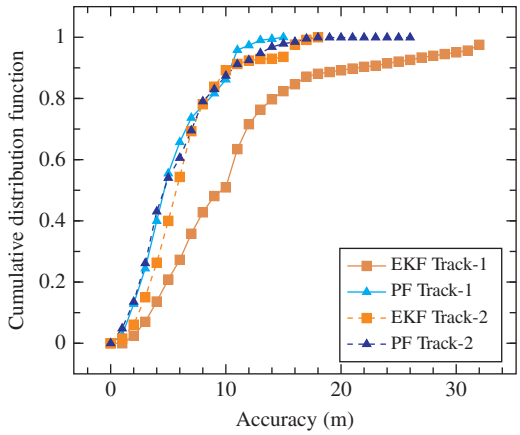

FIG. 13 Cumulative distribution function.

Table 4 Mean Absolute Error for Track-1 and Track-2 Using the PF in GPS+WLAN, GPS-Only, and WLAN-Only Configuration and the EKF

	PF			EKF
	GPS+WLAN	**GPS-Only**	**WLAN-Only**	**GPS+WLAN**
MAE Track 1 (m)	5.36	32.37	6.04	10.72
MAE Track 2 (m)	5.58	6.73	10.46	5.21

clearly outperforms the GPS-only and WLAN-only solutions. The GPS-only solutions fails in estimating Track-1 due the lack of GPS signals. In the case of Track-2, the accuracy of the GPS-only configuration achieves almost the accuracy of the PF filter using pseudoranges and RSS; this suggests that the GPS receiver uses robust methods to estimate the pseudoranges and that the WLAN data does not contribute much to GPS+WLAN solution. The WLAN-only solution performs better on Track-1 than on Track-2, which is reasonable as Track-1 is largely indoors and Track-2 consists of more outdoor sections.

The poor position accuracy of the EKF on Track-1 is due to the unavailability of GPS fixes and because the fingerprint estimates are not trusted sufficiently compared to the pseudoranges. Thus, the weighting between pseudoranges and WLAN position is deficient. Nevertheless, it works fine for Track-2. The PF in contrast performs consistently on both tracks with an average error of 5.5 m. The mechanism to weight pseudoranges and RSS is able to cope with the challenging localization scenario, including a constantly changing sky-view, multipath propagation, and ambiguous fingerprints.

6 Integration of WLAN With Other Data

If WLAN enables the seamless feature, the challenge is the integration with other sensor data in order to yield accurate localization in all environments.

Furthermore, suitable for seamless positioning are all those methods relying on spatially unique sensory data indoors and outdoors such as camera images or RF signals, so that fingerprinting can be applied; or those methods providing uninterrupted reception of sensory data between indoors and outdoors (e.g., source-to-receiver path not blocked by building structures), such as inertial data or magnetic field. A selection of these methods is briefly overviewed in the following subsections.

6.1 Inertial Data

With the development of small and affordable inertial measurement units (IMU) and their proliferation into consumer devices, transforming mobile phones to multisensor platforms, a lot of progress has been made toward seamless positioning. IMUs provide acceleration and angular rate of the device they are attached to and they describe the relative motion of the device through velocity and orientation. These data are independent of the environment and therefore well suited for seamless localization. To integrate inertial data with RSS, recursive Bayesian filters, such as Kalman filters, are applied, where the inertial data are fed into the motion update step. Many schemes to fuse IMU data exist, as it is possible to compute a position relative to the previous position directly from the IMU data. However, such details are out of the scope of this chapter. IMU-assisted WLAN positioning has been addressed, for example, in Jin et al. (2014).

6.2 Vision Navigation

Vision navigation solutions refer to the solutions which rely on images or videos captured by fixed or mobile cameras. A building or a street can be identified also by visual patterns and benchmarks (e.g., a door shape, a tree, etc.), in a similar way with RF-based fingerprinting. The vision navigation relies on comparing visual features collected in an offline training phase with visual captures during the online estimation phase. Visual markers (e.g., paper markers) could be additionally placed in a building to increase the accuracy of the estimates, as done, for example, in Mulloni et al. (2009).

6.3 Visible Light Positioning

Visible light positioning (VLP) is another low-cost positioning method, which relies on line-of-sight (LOS) measurements from light emitting diodes (LED). VLP typically relies on Time of Arrival or Angle of Arrival information and can achieve submeter accuracy. A good overview of various VLP solutions can be found, for example, in Fang et al. (2017).

6.4 Magnetic Field Navigation

Magnetic field navigation is based on the observation that magnetic patterns in various parts of a building have certain characteristic features, which enable a mobile device to recognize its location based on pattern matching or fingerprinting with these magnetic field patterns. Many mobile devices already support magneto-resistive sensors and thus have the capability of doing magnetic field measurements (Nurmi et al., 2017).

6.5 Positioning With Sounds or Ultrasonic Waves

Sound-based positioning systems have been investigated in Hazas and Hopper (2006). By difference with the RF waves, which move at light speed, the sound speed is only about 346 m/s. The sound-based solutions typically rely on Time of Arrival and Angle of Arrival measurements and they are able to offer an increased location privacy to the user. The results reported in Hazas and Hopper (2006) showed cm-level achievable accuracy with an ultrasonic positioning system. The main disadvantages are the need for additional hardware and large and bulky sensors needed at both transmitter and receiver side. Sound-based positioning systems are at the moment rather little investigated or analyzed.

Fig. 14 summarizes how the different systems addressed above can be used with fingerprinting and hybridization. As seen here, most of the systems provide some form of signal strength or intensity which enables fingerprinting for positioning. Afterward any combination of two or more such systems can be in principle hybridized, either at measurement level or at position-estimate level. Examples of hybridization algorithms are enumerated in the last column of Fig. 14.

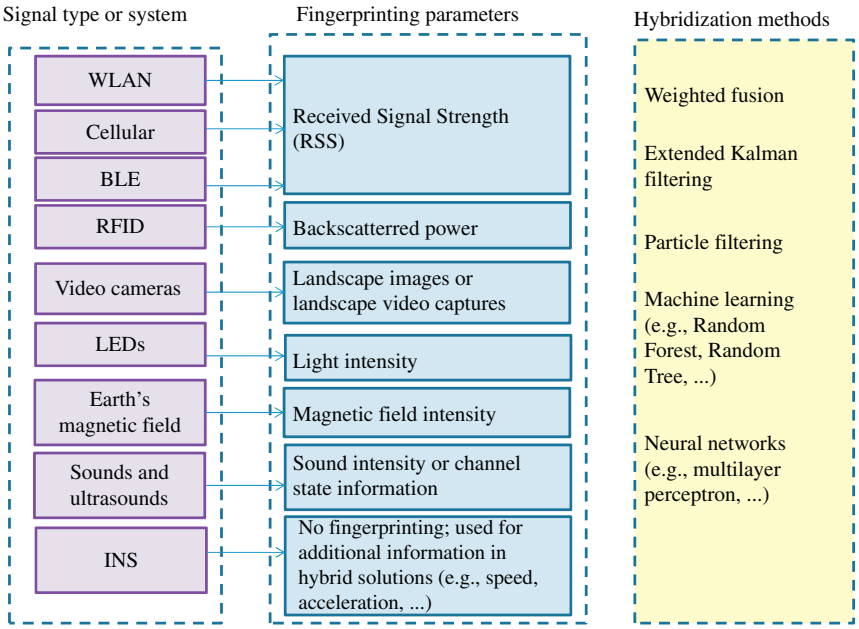

FIG. 14 Summary of hybridization methods based on fingerprinting approaches.

6.6 Multimodal Positioning

From a user perspective, the seamless positioning is not only desired between different environments but between different types of motion as well. Multimodal transportation, meaning that various type of transport is used, such as bike, bus, car, tram, etc., is a typical scenario in urban environments. An example might be a user taking a bus to the train station to travel per train to the next city where he walks or takes a taxi to his destination. In this example the user employs different vehicles, which have all different types of motion. To achieve accurate seamless positioning, these modes of motion need to be appropriately modeled and then detected by the positioning algorithm. The integration of such models with sensory (e.g., RSS) and/or location data is usually achieved by Kalman filter type methods. The interacting multiple model (IMM) algorithm allows further to detect different motions and weights between the outcomes of parallel running Kalman filters which each employ a different motion model (Bar-Shalom et al., 2001). The integration of inertial data into the motion models is particularly beneficial for this approach.

6.7 Cloud Architectures

In order to decrease the computational resources at the mobile side, and thus to increase the mobile battery life, cloud-based solutions such as the cloud GNSS concept

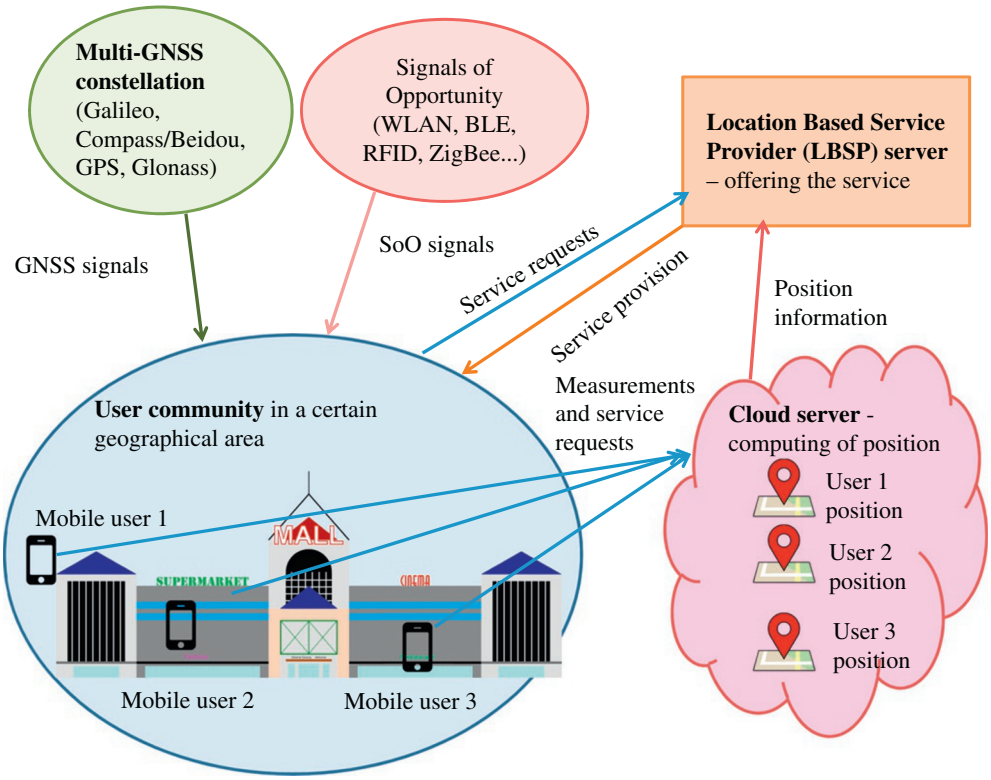

FIG. 15 Cloud positioning concept.

(Lucas-Sabola et al., 2016) are emerging. The concept is illustrated in Fig. 15 and it relies on the idea that various measurements provided by users in a certain geographical areas, such as GNSS pseudoranges, WLAN RSS, etc., are sent to a cloud server. The cloud server uses the information provided by all the users in the area and estimates jointly the user positions. In such a way, a user with clear GNSS signal (e.g., placed outdoors near a shopping mall) can help via his/her measurements the position estimate of the users nearby, who are indoors. The other users' location is not visible to the end users; only the cloud server has access at the full information. Such architectures of course may raise issues of privacy and security of the localization solutions, which are outside the scope of this chapter. The readers interested in more details on the security of location can found a good survey in chapter 3 of Zekavat and Buehrer (2011).

The readers interested in more details about existing navigation methods on smartphones, a very good survey has been recently published in Davidson and Piché (2017).

7 Open Issues and Conclusions

Fingerprinting solutions, typically based on RSS measurements are among the most spread low-cost localization solutions nowadays in indoor and urban areas. In order to achieve seamless localization, one key point is the seamless integration of different fingerprint databases and other navigation solutions, such as GNSS, sensors, etc. The emerging communication systems such as cellular 5G or 802.11az WLAN solutions are moving away from fingerprinting toward ranging solutions, relying more and more heavily on angle and time measurements and on the presence of the line-of-sight. Indeed, future wireless communication networks are expected to be very dense, especially in urban areas where the user location needs are stringent, and to operate in wider bands, thus providing inherently a better location accuracy (Koivisto et al., 2017).

This chapter started with an overview of RSS-based fingerprinting with WLAN signals (see Section 2), which currently are the most widespread indoor and urban wireless channels. The main motivation came from the fact that WLAN signals can be used for positioning with no additional hardware or infrastructures and with only minor software updates at network or mobile side. Typical fingerprinting methods, that can be divided into methods relying on full training database, and methods with reduced training database, such as clustering, path-loss, or image-based approaches, were described.

In the following Section 3, the focus was on various challenges in fingerprinting. The main challenges were summarized (see Table 2) and some of these challenges, such as the effect of RSS offsets, database reduction through different mechanisms and dealing with coverage gaps, were explained in more detail together with their possible solutions.

In Section 4, two studies of combining WLAN signals with BLE and RFID signals were described, respectively in order to take better advantage of existing signals of opportunity. A very simple combining mechanism based on fingerprinting data was employed and it was shown that under some assumptions, such as scarce AP distribution of some systems, adding a second system for the positioning is indeed beneficial.

In addition, seamless positioning solutions that rely on GNSS and WLAN were presented in Section 5. Both systems are available world-wide, infrastructure as well as inexpensive end-user devices that provide pseudoranges (Humphreys et al., 2016), so that more accurate and even ubiquitous localization is achievable with that combination. New developments, such as ultra-dense IoT networks, are supposed to deliver submeter accuracy in a seamless fashion and may provide in combination with GNSS true ubiquitous localization.

Fusing GNSS pseudoranges and RSS signatures in particular (see Section 5.2), can overcome the drawbacks that GNSS presents as a ranging-based system. Because WLAN fingerprinting is to some extent complementary to GNSS and it can enhance information of GNSS more than WLAN ranging-based methods. The different error mechanisms of GNSS and WLAN fingerprinting also invite to develop GNSS multipath detection and mitigation strategies. However, ubiquitous localization with that approach requires ubiquity of fingerprint databases with a harmonized access and datasets.

Finally, Section 6 discussed more at large the different hybridization options existing nowadays for seamless positioning and what are other potential systems which can be used for an increased accuracy and/or availability of the positioning estimates.

To conclude, it is the authors' belief that seamless positioning can be achieved only by adequate combining or hybridization of different existing solutions, rather than inventing a new system equally good for indoor and outdoor solutions. With the advent of cheaper and lower complexity GNSS solutions, such as cloud GNSS solutions, it is very likely that future seamless localization systems will have a cloud component, partly relying on GNSS data, and a user-centric component, relying on low-cost easily accessible measurements such as various signal strengths.

References

Abdou, A.S., Aziem, M.A., Aboshosha, A., 2016. An efficient indoor localization system based on affinity propagation and support vector regression. In: 2016 Sixth International Conference on Digital Information Processing and Communications (ICDIPC).

Agarwal, P., Burgard, W., Stachniss, C., 2014. Survey of geodetic mapping methods: geodetic approaches to mapping and the relationship to graph-based SLAM. IEEE Robot. Autom. Mag. 21 (3), 63–80. https://doi.org/10.1109/MRA.2014.2322282.

Bar-Shalom, Y., Li, X.-R., Kirubarajan, T., 2001. Estimation with Applications to Tracking and Navigation. John Wiley & Sons, Inc..

Cadena, C., Carlone, L., Carrillo, H., Latif, Y., Scaramuzza, D., Neira, J., Reid, I., Leonard, J.J., 2016. Past, present, and future of simultaneous localization and mapping: toward the robust-perception age. IEEE Trans. Robot. 32 (6), 1309–1332. https://doi.org/10.1109/TRO.2016.2624754.

Chen, Q., Wang, B., 2015. FinCCM: fingerprint crowdsourcing, clustering and matching for indoor subarea localization. IEEE Wireless Commun. Lett. 4 (6), 677–680. https://doi.org/10.1109/LWC.2015.\break{}2482971.

Chen, Y.-C., Chiang, J.-R., Chu, H.-H., Huang, P., Tsui, A.W., 2005. Sensor-assisted WiFi indoor location system for adapting to environmental dynamics. In: Proceedings of 8th ACM International Symposium on Modeling, Analysis and Simulation of Wireless and Mobile Systems, pp. 118–125.

Chen, W., Chang, Q., Hou, H.-T., Wang, W.-P., 2006. Power-efficient access-point selection for indoor location estimation. IEEE Trans. Knowl. Data Eng. 18 (7), 877–888.

Cheng, W., Tan, K., Omwando, V., Zhu, J., Mohapatra, P., 2013. RSS-ratio for enhancing performance of RSS-based applications. In: Proceedings of IEEE INFOCOM, pp. 3075–3083.

Coluccia, A., Ricciato, F., Ricci, G., 2014. Positioning based on signals of opportunity. IEEE Commun. Lett. 18 (2), 356–359. https://doi.org/10.1109/LCOMM.2013.123013.132297.

Cramariuc, A., Huttunen, H., Lohan, E.S., 2016. Clustering benefits in mobile-centric WiFi positioning in multi-floor buildings. In: 2016 International Conference on Localization and GNSS (ICL-GNSS).

Davidson, P., Piché, R., 2017. A survey of selected indoor positioning methods for smartphones. IEEE Commun. Surv. Tutorials 19 (2), 1347–1370. https://doi.org/10.1109/COMST.2016.2637663.

DeCuir, J., 2014. Introducing Bluetooth Smart: Part I: A look at both classic and new technologies. IEEE Consumer Electron. Mag. 3 (1), 12–18. https://doi.org/10.1109/MCE.2013.2284932.

Della Rosa, F., Leppäkoski, H., Biancullo, S., Nurmi, J., 2010a. Ad-hoc networks aiding indoor calibrations of heterogeneous devices for fingerprinting applications. In: Proceedings of International Conference on Indoor Positioning and Indoor Navigation (IPIN).

Della Rosa, F., Paakki, T., Leppäkoski, H., Nurmi, J., 2010b. A cooperative framework for path loss calibration and indoor mobile positioning. In: Proceedings of 7th Workshop on Positioning Navigation and Communication (WPNC), Dresden, Germany.

Fang, S.-H., Lin, T.-N., 2012. Principal component localization in indoor WLAN environments. IEEE Trans. Mob. Comput. 11 (1), 100–110.

Fang, J., Yang, Z., Long, S., Wu, Z., Zhao, X., Liang, F., Jiang, Z.L., Chen, Z., 2017. High-speed indoor navigation system based on visible light and mobile phone. IEEE Photonics J. 9 (2), 1–11. https://doi.org/10.1109/JPHOT.2017.2687947.

Feng, C., Au, W.S.A., Valaee, S., Tan, Z., 2012. Received-signal-strength-based indoor positioning using compressive sensing. IEEE Trans. Mob. Comput. 11 (12), 1983–1993. https://doi.org/10.1109/TMC.2011.216.

Haeberlen, A., Rudys, A., Flannery, E., Wallach, D.S., Ladd, A.M., Kavraki, L.E., 2004. Practical robust localization over large-scale 802.11 wireless networks. In: Proceedings of 10th Annual International Conference on Mobile Computing and Networking (MOBICOM).

Hasani, M., Talvitie, J., Sydänheimo, L., Lohan, E.S., Ukkonen, L., 2015. Hybrid WLAN-RFID indoor localization solution utilizing textile tag. IEEE Antennas Wirel. Propag. Lett. 14, 1358–1361. https://doi.org/10.1109/LAWP.2015.2406951.

Hazas, M., Hopper, A., 2006. Broadband ultrasonic location systems for improved indoor positioning. IEEE Trans. Mob. Comput. 5 (5), 536–547. https://doi.org/10.1109/TMC.2006.57.

Hejc, G., Seitz, J., Vaupel, T., 2014. Bayesian sensor fusion of Wi-Fi signal strengths and GNSS code and carrier phases for positioning in urban environments. In: IEEE/ION Position, Location and Navigation Symposium—PLANS 2014, pp. 1026–1032.

Hossain, A.K.M.M., Jin, Y., Soh, W.-S., Van, H.N., 2013. SSD: a robust RF location fingerprint addressing mobile devices' heterogeneity. IEEE Trans. Mob. Comput. 12 (1), 65–77.

Humphreys, T.E., Murrian, M., van Diggelen, F., Podshivalov, S., Pesyna, K.M., 2016. On the feasibility of cm-accurate positioning via a smartphone's antenna and GNSS chip. In: 2016 IEEE/ION Position, Location and Navigation Symposium (PLANS), pp. 232–242.

Jia, M., Yang, Y., Kuang, L., Xu, W., Chu, T., Song, H., 2016. An indoor and outdoor seamless positioning system based on android platform. In: 2016 IEEE Trustcom/BigDataSE/ISPA, pp. 1114–1120.

Jin, M., Koo, B., Lee, S., Park, C., Lee, M.J., Kim, S., 2014. IMU-assisted nearest neighbor selection for real-time WiFi fingerprinting positioning. In: 2014 International Conference on Indoor Positioning and Indoor Navigation (IPIN), pp. 745–748.

Jung, S.H., Moon, B.C., Han, D., 2017. Performance evaluation of radio map construction methods for Wi-Fi positioning systems. IEEE Trans. Intell. Transp. Syst. 18 (4), 880–889. https://doi.org/10.1109/TITS.2016.2594479.

Kaemarungsi, K., 2006. Distribution of WLAN received signal strength indication for indoor location determination. In: Proceedings of 1st International Symposium on Wireless Pervasive Computing.

Karttunen, A., Gustafson, C., Molisch, A.F., Wang, R., Hur, S., Zhang, J., Park, J., 2016. Path loss models with distance-dependent weighted fitting and estimation of censored path loss data. IET Microwaves Antennas Propag. 10 (14), 1467–1474. https://doi.org/10.1049/iet-map.2016.0042.

Kasebzadeh, P., Granados, G.S., Lohan, E.S., 2014. Indoor localization via WLAN path-loss models and Dempster-Shafer combining. In: International Conference on Localization and GNSS 2014 (ICL-GNSS 2014).

Khullar, R., Dong, Z., 2017. Indoor localization framework with WiFi fingerprinting. In: 2017 26th Wireless and Optical Communication Conference (WOCC).

Kjaergaard, M.B., 2006. Automatic mitigation of sensor variations for signal strength based location systems. In: Proceedings of Second International Workshop on Location and Context Awareness.

Kjaergaard, M.B., Munk, C.V., 2008. Hyperbolic location fingerprinting: a calibration-free solution for handling differences in signal strength. In: Proceedings of Sixth Annual International Conference on Pervasive Computing and Communications, pp. 110–116.

Koivisto, M., Costa, M., Werner, J., Heiska, K., Talvitie, J., Leppänen, K., Koivunen, V., Valkama, M., 2017. Joint device positioning and clock synchronization in 5G ultra-dense networks. IEEE Trans. Wirel. Commun. 16 (5), 2866–2881. https://doi.org/10.1109/TWC.2017.2669963.

Kotaru, M., Joshi, K., Bharadia, D., Katti, S., 2015. SpotFi: Decimeter level localization using WiFi. SIGCOMM Comput. Commun. Rev. 45 (4), 269–282. https://doi.org/10.1145/2829988.2787487.

Kushki, A., Plataniotis, K.N., Venetsanopoulos, A.N., 2007. Kernel-based positioning in wireless local area networks. IEEE Trans. Mob. Comput. 6 (6), 689–705.

Laitinen, E., 2017. Physical layer challenges and solutions in seamless positioning via GNSS, cellular and WLAN systems. Ph.D. thesis, Tampere University of Technology, Tampere, Finland.

Laitinen, E., Lohan, E.S., 2016. On the choice of access point selection criterion and other position estimation characteristics for WLAN-based indoor positioning. MDPI Sens. 16 (5).

Laitinen, E., Lohan, E.S., Talvitie, J., Shrestha, S., 2012. Access point significance measures in WLAN-based location. In: Proceedings of 9th Workshop on Positioning Navigation and Communication (WPNC), Dresden, Germany, pp. 24–29.

Laitinen, E., Talvitie, J., Lohan, E.S., 2015. On the RSS biases in WLAN-based indoor positioning. In: Proceedings of IEEE International Communication Workshop (ICCW), London, UK, pp. 797–802.

Li, B., O'Keefe, K., 2013. WLAN TOA ranging with GNSS hybrid system for indoor navigation. In: Proceedings of the 26th International Technical Meeting of the Satellite Division of the Institute of Navigation, pp. 416–425.

Liang, D., Zhang, Z., Peng, M., 2015. Access point reselection and adaptive cluster splitting-based indoor localization in wireless local area networks. IEEE Internet Things J. 2 (6), 573–585.

Lin, H., Chen, L., 2016. An optimized fingerprint positioning algorithm for underground garage environment. In: 2016 International Conference on Information Networking (ICOIN), pp. 291–296.

Liu, H., Darabi, H., Banerjee, P., Liu, J., 2007. Survey of wireless indoor positioning techniques and systems. IEEE Trans. Syst. Man Cybern. 37 (6), 1067–1080.

Liu, W., Fu, X., Deng, Z., Xu, L., Jiao, J., 2016. Smallest enclosing circle-based fingerprint clustering and modified-WKNN matching algorithm for indoor positioning. In: 2016 International Conference on Indoor Positioning and Indoor Navigation (IPIN).

Liu, S., Si, P., Xu, M., He, Y., Zhang, Y., 2017. Edge big data-enabled low-cost indoor localization based on Bayesian analysis of RSS. In: 2017 IEEE Wireless Communications and Networking Conference (WCNC).

Lohan, E.S., Koski, K., Talvitie, J., Ukkonen, L., 2014. WLAN and RFID Propagation channels for hybrid indoor positioning. In: International Conference on Localization GNSS 2014 (ICL-GNSS 2014). IEEE.

Lucas-Sabola, V., Seco-Granados, G., López-Salcedo, J.A., García-Molina, J.A., Crisci, M., 2016. Cloud GNSS receivers: new advanced applications made possible. In: 2016 International Conference on Localization and GNSS (ICL-GNSS).

Machaj, J., Brida, P., Piché, R., 2011. Rank based fingerprinting algorithm for indoor positioning. In: Proceedings of International Conference on Indoor Positioning and Indoor Navigation (IPIN).

Miao, H., Wang, Z., Wang, J., Zhang, L., Zhengfeng, L., 2014. A novel access point selection strategy for indoor location with Wi-Fi. In: Proceedings of Control and Decision Conference (CCDC), Changsha, China, pp. 5260–5265.

Milioris, D., Tzagkarakis, G., Jacquet, P., Tsakalides, P., 2011. Indoor positioning in wireless LANS using compressive sensing signal-strength fingerprints. In: 2011 19th European Signal Processing Conference, pp. 1776–1780.

Mo, Y., Zhang, Z., Meng, W., Agha, G., 2015. Space division and dimensional reduction methods for indoor positioning system. In: 2015 IEEE International Conference on Communications (ICC), pp. 3263–3268.

Moreira, A., Nicolau, M.J., Costa, A., Meneses, F., 2016. Indoor tracking from multidimensional sensor data. In: 2016 International Conference on Indoor Positioning and Indoor Navigation (IPIN).

Mulloni, A., Wagner, D., Barakonyi, I., Schmalstieg, D., 2009. Indoor positioning and navigation with camera phones. IEEE Pervasive Comput. 8 (2), 22–31. https://doi.org/10.1109/MPRV.2009.30.

Munir, H., Hassan, S.A., Pervaiz, H., Ni, Q., Musavian, L., 2017. Resource optimization in multi-tier HetNets exploiting multi-slope path loss model. IEEE Access 5, 8714–8726. https://doi.org/10.1109/ACCESS.2017.2699941.

Nur, K., Feng, S., Ling, C., Ochieng, W., 2013. Integration of GPS with a WiFi high accuracy ranging functionality. Geo-spatial Inform. Sci. 16 (3), 155–168. https://doi.org/10.1080/10095020.2013.817106.

Nurmi, J., Lohan, E.S., Wymeersch, H., Seco-Granados, G., Nykanen, O. (Eds.), 2017. Multi-Technology Positioning. Springer.

Pasku, V., Angelis, A.D., Angelis, G.D., Arumugam, D.D., Dionigi, M., Carbone, P., Moschitta, A., Ricketts, D.S., 2017. Magnetic field-based positioning systems. IEEE Commun. Surv. Tutorials 19 (3), 2003–2017. https://doi.org/10.1109/COMST.2017.2684087.

Rasmussen, C.E., Williams, C.K.I., 2006. Gaussian Processes for Machine Learning. MIT Press.

Razavi, A., Valkama, M., Lohan, E.S., 2015. K-means fingerprint clustering for low-complexity floor estimation in indoor mobile localization. In: 2015 IEEE Globecom Workshops (GC Wkshps).

Richter, P., Toledano-Ayala, M., 2015. Revisiting Gaussian process regression modeling for localization in wireless sensor networks. Sensors 15 (9), 22587–22615. https://doi.org/10.3390/s150922587.

Richter, P., Toledano-Ayala, M., 2017. Ubiquitous and seamless localization: fusing GNSS pseudoranges and WLAN signal strengths. Mob. Inf. Syst. 2017, 16, Article ID 8260746. https://doi.org/10.1155/2017/8260746.

Richter, P., Toledano-Ayala, M., Soto-Zarazúa, G.M., Rivas-Araiza, E.A., 2014. A survey of hybridisation methods of GNSS and wireless LAN based positioning system. J. Ambient Intell. Smart Environ. 6 (6), 723–738. https://doi.org/10.3233/AIS-140289.

Ristic, B., Arulampalam, S., Gordon, N., 2004. Beyond the Kalman Filter: Particle Filters for Tracking Applications. Artech House Publishers.

Schwaighofer, A., Grigoras, M., Tresp, V., Hoffmann, C., 2004. GPPS: a Gaussian process positioning system for cellular networks. In: Thrun, S., Saul, L.K., Schölkopf, B.P. (Eds.) Advances in Neural Information Processing Systems 16. MIT Press, Cambridge, MA, pp. 579–586.

Shrestha, S., Talvitie, J., Lohan, E.S., 2013. Deconvolution-based indoor localization with WLAN signals and unknown access point locations. In: 2013 International Conference on Localization and GNSS (ICL-GNSS).

Shu, Y., Bo, C., Shen, G., Zhao, C., Li, L., Zhao, F., 2015. Magicol: indoor localization using pervasive magnetic field and opportunistic WiFi sensing. IEEE J. Sel. Areas Commun. 33 (7), 1443–1457. https://doi.org/10.1109/JSAC.2015.2430274.

Sun, G., Chen, J., Guo, W., Liu, K.J.R., 2005. Signal processing techniques in network-aided positioning: a survey of state-of-the-art positioning designs. IEEE Signal Process. Mag. 22 (4), 12–23. https://doi.org/10.1109/MSP.2005.1458273.

Talvitie, J., Lohan, E.S., Renfors, M., 2014. The effect of coverage gaps and measurement inaccuracies in fingerprinting based indoor localization. In: International Conference on Localization and GNSS 2014 (ICL-GNSS 2014).

Talvitie, J., Renfors, M., Lohan, E.S., 2015. Distance-based interpolation and extrapolation methods for RSS-based localization with indoor wireless signals. IEEE Trans. Veh. Technol. 64 (4), 1340–1353. https://doi.org/10.1109/TVT.2015.2397598.

Talvitie, J., Renfors, M., Lohan, E.S., 2016. Novel indoor positioning mechanism via spectral compression. IEEE Commun. Lett. 20 (2), 352–355. https://doi.org/10.1109/LCOMM.2015.2504097.

Taylor, C.N., Veth, M.J., Raquet, J.F., Miller, M.M., 2011. Comparison of two image and inertial sensor fusion techniques for navigation in unmapped environments. IEEE Trans. Aerosp. Electron. Syst. 47 (2), 946–958. https://doi.org/10.1109/TAES.2011.5751236.

Torres-Sospedra, J., Montoliu, R., Trilles, S., Belmonte, O., Huerta, J., 2015. Comprehensive analysis of distance and similarity measures for Wi-Fi fingerprinting indoor positioning systems. Expert Syst. Appl. 42 (23), 9263–9278. https://doi.org/10.1016/j.eswa.2015.08.013.

Uddin, M.T., Islam, M.M., 2015. Extremely randomized trees for Wi-Fi fingerprint-based indoor positioning. In: 2015 18th International Conference on Computer and Information Technology (ICCIT), pp. 105–110.

Varzandian, S., Zakeri, H., Ozgoli, S., 2013. Locating WiFi access points in indoor environments using non-monotonic signal propagation model. In: 2013 9th Asian Control Conference (ASCC).

Vaupel, T., Seitz, J., Kiefer, F., Haimerl, S., Thielecke, J., 2010. Wi-Fi positioning: system considerations and device calibration. In: Proceedings of Indoor Positioning and Indoor Navigation (IPIN).

Wang, L., Wong, W.-C., 2014. A novel rss model and power-bias mitigation algorithm in fingerprinting-based indoor localization in wireless local area networks. In: Proceedings of 20th European Wireless Conference, Barcelona, Spain.

Wang, B., Chen, Q., Yang, L.T., Chao, H.C., 2016. Indoor smartphone localization via fingerprint crowdsourcing: challenges and approaches. IEEE Wirel. Commun. 23 (3), 82–89. https://doi.org/10.1109/MWC.2016.7498078.

Xiao, C., Yang, D., Chen, Z., Tan, G., 2017. 3-D BLE indoor localization based on denoising autoencoder. IEEE Access 5, 12751–12760. https://doi.org/10.1109/ACCESS.2017.2720164.

Yedavalli, K., Krishnamachari, B., Ravula, S., Srinivasan, B., 2005. Ecolocation: a sequence based technique for RF localization in wireless sensor networks. In: IPSN 2005. Fourth International Symposium on Information Processing in Sensor Networks, 2005, pp. 285–292.

Youssef, M.A., Agrawala, A., Shankar, A.U., 2003. WLAN location determination via clustering and probability distributions. In: Proceedings of Pervasive Computing and Communications, Fort Worth, TX, USA, pp. 143–150.

Zekavat, R., Buehrer, R.M. (Eds.), 2011. Handbook of Position Location: Theory, Practice and Advances. Wiley.

Zhang, C., Subbu, K.P., Luo, J., Wu, J., 2015. GROPING: Geomagnetism and cROwdsensing Powered Indoor Navigation. IEEE Trans. Mob. Comput. 14 (2), 387–400. https://doi.org/10.1109/TMC.2014.2319824.

Zhou, Y., Chen, X., Zeng, S., Liu, J., Liang, D.A., 2013. AP selection algorithm in WLAN indoor localization. Inform. Technol. J. 12, 3773–3776.

Zou, H., Luo, Y., Lu, X., Jiang, H., Xie, L., 2015. A mutual information based online access point selection strategy for WiFi indoor localization. In: Proceedings of International Conference on Automation Science and Engineering (CASE), Gothenburg, Sweden, pp. 180–185.

Zou, H., Huang, B., Lu, X., Jiang, H., Xie, L., 2016. A robust indoor positioning system based on the procrustes analysis and weighted extreme learning machine. IEEE Trans. Wirel. Commun. 15 (2), 1252–1266. https://doi.org/10.1109/TWC.2015.2487963.